VI. APPLIED PLASMA RESEARCH

A. Active Plasma Systems

Academic and Research Staff

Prof. L. D. Smullin
Prof. A. Bers
Dr. R. R. Parker

Graduate Students

N. J. Fisch
S. P. Hirshman
C. F. F. Karney
J. L. Kulp
R. K. Linford
M. D. Simonutti
M. S. Tekula
A. E. Throop
D. C. Watson

1. USE OF MACSYMA IN THE SYMBOLIC DERIVATION OF NONLINEAR COUPLING COEFFICIENTS

National Science Foundation (Grant GK-37979X)

C. F. F. Karney, A. Bers

Introduction

In a previous report[1] we considered the excitation of ion acoustic, electrostatic ion cyclotron, and magnetosonic waves by a strong pump near the lower hybrid frequency in a highly magnetized uniform plasma ($\omega_{pi} = 10\ \Omega_i$, $\Omega_e \approx 4.5\ \omega_{pe}$). We described the derivation of coupling coefficients for two particular cases, (i) the pump at the lower hybrid frequency coupling to two low-frequency (ion acoustic) waves and (ii) the pump and an idler above the low hybrid coupling to a single low-frequency (electrostatic ion cyclotron or magnetosonic) wave. In this report we describe computational methods for deriving coupling coefficients by using the facilities of MACSYMA.[2] There are two advantages to deriving such expressions on MACSYMA. First, once the technique has been developed, it should be relatively simple to apply it to new problems and to obtain approximate answers in a short time. Second, with little additional effort on the part of the user corrections to the dominant terms can be derived. This provides a useful check on the accuracy of the approximations.

In the nonlinear coupling-of-modes theory we look for three waves such that

$$\omega_n = \omega_a + \omega_b \tag{1}$$

$$\bar{k}_n = \bar{k}_a + \bar{k}_b. \tag{2}$$

We then calculate the second-order current[3] $J^{(2)}_{a,b}$ arising from the nonlinear

interaction of modes a and b. This current is considered as a perturbing current to mode n. The perturbation may be expressed in terms of the coupling coefficient M, where

$$M = \frac{E_n J^{(2)}_{a,b}}{\omega_n}. \tag{3}$$

In this problem we take mode n to be the ion mode that we are trying to excite; a is the pump and b is the idler. Note that, since the pump is normally at the highest frequency, we have $\omega_b < 0$.

We assume that the plasma is infinite and homogeneous, and that the magnetic field is uniform. We take the ions to be cold, and consider only modes described by the electrostatic approximation. We take $\omega_{LH} = \omega_{pi}$, since $\Omega_e^2 \gg \omega_{pe}^2$.

For work with MACSYMA, we have normalized a number of quantities in order to avoid having a large number of common factors. Also, since we use the electrostatic approximation, $\bar{E}$ has been replaced by $\frac{|\bar{E}|}{|\bar{k}|}\bar{k}$.

$$\text{Frequency:} \quad WN = \omega/\Omega_i \tag{4}$$

$$\text{Wave numbers:} \quad KN = \bar{k}c_s/\Omega_i$$

$$KNM = |KN| \tag{5}$$

$$KNX = k_x c_s/\Omega_i, \quad \text{etc.}$$

$$\text{Conductivity SIGMAN:} = \frac{\bar{\bar{\sigma}}\Omega_i}{i\epsilon_o \omega_{pi}^2} \tag{6}$$

$$\left.\begin{matrix} VE \\ VI \end{matrix}\right\} = SIGMAN.KN$$

$$\left.\begin{matrix} VET \\ VIT \end{matrix}\right\} = \text{Transpose} \left\{\begin{matrix} VE \\ VI \end{matrix}\right\} \tag{7}$$

$$\left.\begin{matrix} NE \\ NI \end{matrix}\right\} = \frac{KN.\left\{\begin{matrix} VE \\ VI \end{matrix}\right\}}{WN} \tag{8}$$

All of the common factors of the terms in the resulting expression for M are combined and called CONSTFACT. The terms in M are shown in Fig. VI-1.

(C3) DISPLAY(CONSTFACT,MICONV,MIFLOW,MECONV,MEFLOW,MEPRES,MECONT,M)$

$$\text{(E4)}\qquad \text{CONSTFACT} = \frac{E_A\, E_B\, E^*_N\, EP_O\, WN_{PI}^2\, Q}{KNM_A\, KNM_B\, W_{CI}\, MI\, KNM_N\, C_S}$$

$$\text{(E5)}\qquad \text{MICONV} = -\frac{(KN_A \cdot VI_B)\,(VIT_N \cdot VI_A) + (KN_B \cdot VI_A)\,(VIT_N \cdot VI_B)}{2\, WN_N}$$

$$\text{(E6)}\qquad \text{MIFLOW} = -\frac{NI_B\,(KN_N \cdot VI_A) + NI_A\,(KN_N \cdot VI_B)}{2\, WN_N}$$

$$\text{(E7)}\qquad \text{MECONV} = \frac{(KN_A \cdot VE_B)\,(VET_N \cdot VE_A) + (KN_B \cdot VE_A)\,(VET_N \cdot VE_B)}{2\, MU\, WN_N}$$

$$\text{(E8)}\qquad \text{MEFLOW} = \frac{NE_B\,(KN_N \cdot VE_A) + NE_A\,(KN_N \cdot VE_B)}{2\, WN_N}$$

$$\text{(E9)}\qquad \text{MEPRES} = -\frac{NE_A\, NE_B\,(VET_N \cdot KN_N)}{2\, WN_N}$$

$$\text{(E10)}\qquad \text{MECONT} = \frac{NE_B\,(KN_N \cdot VE_A)\,(VET_N \cdot \frac{KN_N}{WN_N}) + NE_A\,(KN_N \cdot VE_B)\,(VET_N \cdot \frac{KN_N}{WN_N})}{2\, WN_N}$$

(E11)
$$M = \text{CONSTFACT}\,(\text{MECONT} + \text{MECONV} + \text{MEFLOW} + \text{MEPRES} + \text{MICONV} + \text{MIFLOW})$$

TIME= 40 MSEC.

Fig. VI-1. Coupling coefficient M expressed in terms of MACSYMA variables.

Outline of Method

The key to symbolic derivation of approximate expressions is the MACSYMA TAYLOR function. TAYLOR (exp, var, pt, pow) expands exp in a truncated Taylor's series in the variable var around the point pt. Terms through (var-pt)**pow are generated. This enables the user to order quite general expressions in terms of some small parameter and truncate it at any specified level. The result is put in a special internal form so that the many operations on the results preserve the structure and truncation level. Figure VI-2 shows some examples of the use of this command. The Command lines entered by the user begin (Cn) and the result is Displayed in lines (Dn). The aim in working with Taylor's series is usually to keep the number of significant terms constant. This means that the truncation level may have to be removed or reset when working with expressions whose leading terms are of higher order than 1. It is not always known how the truncation level should be set in a new problem, and in such a case it may be necessary to go back and readjust the level after the first attempt.

In any physical problem, then, we must look for large and small parameters, in which we can order the terms of our expression. For instance, in problems involving a lower hybrid wave coupling to an ion acoustic wave we might wish to say that the mass ratio $\frac{m_i}{m_e} \triangleq \mu$ is large, the phase velocity of the lower hybrid wave $\frac{\omega/k}{c_s} \triangleq \frac{1}{\epsilon}$ is large,

```
(C3) S1:SQRT(4-5*SIN(X))*COSH(X);
TIME= 66 MSEC.
(D3)                COSH(X) SQRT(4 - 5 SIN(X))

(C4) T1:TAYLOR(S1,X,0,3);
TIME= 607 MSEC.
```

(D4) $$2 - \frac{5X}{4} + \frac{39X^2}{64} - \frac{1015X^3}{1536} + \ldots$$

```
(C5) T1^2;
TIME= 189 MSEC.
```

(D5) $$4 - 5X + 4X^2 - \frac{25X^3}{6} + \ldots$$

Here we see the contagious effects of the Taylor series representation. Adding T1 and S2 converts S2 from the general representation in which it was entered to the special representation used by Taylor series. Note the one consequence of this is the loss of the X^4/3 term of S2.

```
(C6) S2:X+X^2+X^4/3;
TIME= 47 MSEC.
```

(D6) $$X + X^2 + \frac{X^4}{3}$$

```
(C7) T1+S2;
TIME= 158 MSEC.
```

(D7) $$2 - \frac{X}{4} + \frac{103X^2}{64} - \frac{1015X^3}{1536} + \ldots$$

There are a number of ways we can prevent truncation occuring, two of which are shown here. EV just removes the information about the truncation level, whereas RATDISREP converts an expression into the general representation.

```
(C8) EV(T1)+S2;
TIME= 304 MSEC.
```

(D8) $$\frac{3072 - 384X + 2472X^2 - 1015X^3 + 512X^4}{1536}$$

```
(C9) RATDISREP(T1)+S2;
TIME= 107 MSEC.
```

(D9) $$2 - \frac{X}{4} + \frac{103X^2}{64} - \frac{1015X^3}{1536} + \frac{X^4}{3}$$

This is a case where, because the leading term is not of order 1, care must be taken to adjust the truncation level correctly. This may either be accomplished by removing the truncation level (C13), or by resetting it (C14). Comparison with D15 shows that in either case the expression is correct to 3 significant terms (the number of terms in the original Taylor series D11).

```
(C10) S3:8*X^3/SQRT(1-3*TAN(X));
TIME= 83 MSEC.
```

(D10) $$\frac{8X^3}{\mathrm{SQRT}(1 - 3\,\mathrm{TAN}(X))}$$

```
(C11) T3:TAYLOR(S3,X,0,5);
TIME= 1127 MSEC.
```

(D11) $$8X^3 + 12X^4 + 27X^5 + \ldots$$

```
(C12) T3^2;
TIME= 186 MSEC.
(D12)                0

(C13) EV(T3)^2;
TIME= 117 MSEC.
```

(D13) $$64X^6 + 192X^7 + 576X^8 + 648X^9 + 729X^{10}$$

```
(C14) TAYLOR(T3,X,0,8)^2;
TIME= 365 MSEC.
```

(D14) $$64X^6 + 192X^7 + 576X^8 + \ldots$$

```
(C15) TAYLOR(S3^2,X,0,10);
TIME= 5278 MSEC.
```

(D15) $$64X^6 + 192X^7 + 576X^8 + 1792X^9 + 5568X^{10} + \ldots$$

Fig. VI-2. Examples of the use of TAYLOR function and manipulation of Taylor's series in MACSYMA.

and $\cos\theta \overset{\Delta}{=} \epsilon_2$ for the lower hybrid wave is small.

In order to invoke the Taylor's series routine, we must combine these parameters into a single one, with due regard for the weight of various parameters. So we might write

$$\frac{m_i}{m_e} = \mu = \frac{1}{\delta^2} \tag{9}$$

$$kc_s/\omega = \epsilon_1 = \lambda_1\delta \tag{10}$$

$$\cos\theta = \epsilon_2 = \lambda_2\delta, \tag{11}$$

where $\lambda_1, \lambda_2 \sim 1$. We may then proceed to take Taylor's series in δ about zero. At the end we need only substitute for δ, λ_1 and λ_2 to recover the original parameters μ, ϵ_1 and ϵ_2. The weighting given to the small or large parameters need not have any physical significance. The reason for assigning weights is merely to tell the Taylor's series routine how to truncate the expressions. At any stage we may recover the original parameters by substituting for the λ. In general, the λ may take fairly large or small values, but the aim is to have

$$\delta \ll \lambda_{a,\,b,\,c} \ll \lambda_{m,\,n,\,o} \approx 1 \ll \lambda_{x,\,y,\,z} \ll \frac{1}{\delta},$$

so that within each coefficient of δ there is a further and more fine ordering in the λ. If such a fine ordering is eventually used, however, the Taylor's series truncation, originally based on the order of δ, may have to be modified.

Coupling to Two Ion Acoustic Modes

Consider a small k pump mode at the lower hybrid frequency (dispersion relation $\omega = \omega_{LH} \approx \omega_{pi}$) coupling to two ion acoustic wave modes b and n at approximately half the lower hybrid frequency (dispersion relation $\omega^2 = k^2c_s^2$). The pump propagates nearly perpendicular to the magnetic field. A typical case in k space is illustrated in Fig. VI-3. (In

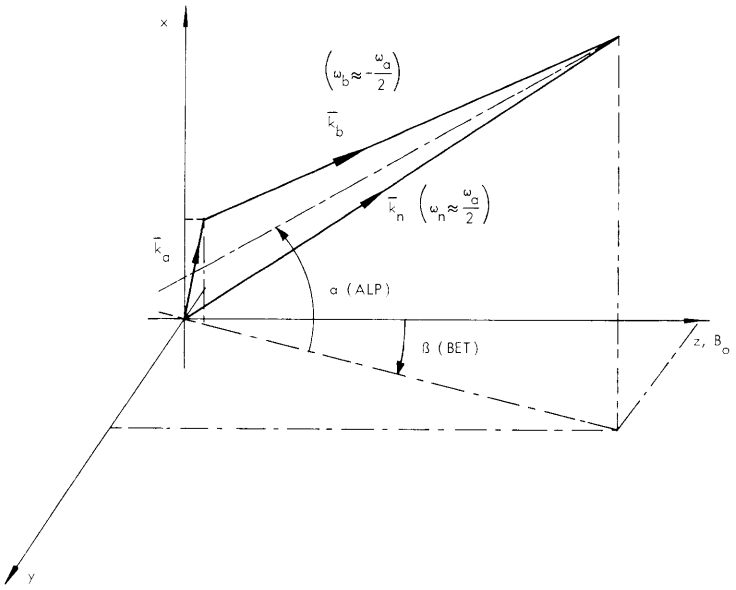

Fig. VI-3.
Typical $\bar{k}$ space diagram for the case of one lower hybrid mode (a) coupling to two ion acoustic modes (b and n).

choosing a coordinate system we make $k_{ay} = 0$.) The small parameters that we choose are the following.

$$k_{ax}c_s/\omega_a = \epsilon_1 = \lambda_1\delta; \qquad \text{KNX[A]: LM1*DEL*WN[A]} \tag{12}$$

$$\frac{k_{az}}{k_{ax}} = \epsilon_2 = \lambda_2\delta; \quad \text{KNZ[A]:LM1*LM2*DEL↑2*WN[A]} \tag{13}$$

$$\frac{\Omega_i}{\omega_a} = \epsilon_3 = \lambda_2\delta; \quad \text{WN[CI]:LM3*DEL*WN[A]} \tag{14}$$

$$\frac{\omega_a}{\Omega_e} = \epsilon_4 = \lambda_4\delta^2; \quad \text{WN[CE]:WN[A]/DEL↑2/LM4} \tag{15}$$

$$\frac{m_e}{m_i} = \frac{1}{\mu} = \delta^2; \quad \text{MU:1/DEL↑2.} \tag{16}$$

On the right-hand side of these expressions we have shown the commands that give MACSYMA this information. Note that in defining the MACSYMA variables we compared frequencies and wave numbers to WN[A]. TAYLOR will, in effect, assume that all undefined frequencies and wave numbers are of the same order as WN[A].

Figure VI-4 shows the steps in the calculation of the ion terms of the coupling coefficient. A similar set of MACSYMA commands accomplishes the same calculation for the electrons. Note that as a consequence of the cancellation of the leading terms it is necessary to carry 3 significant terms throughout the calculation to be able to obtain 2 terms in the answer.

The resultant expressions for M are

$$M_{ion} = C\left\{-\frac{(1-2\sin^2\alpha)}{2}\left(\frac{k_a c_s}{\omega_a}\right)^2 - 10i\,\frac{\cos\alpha\,\sin\alpha\,\sin\beta}{2}\left(\frac{k_a c_s}{\omega_a}\right)^2\frac{\Omega_i}{\omega_a}\right\} \tag{17}$$

$$M_{el} = C\left\{-\left(\frac{k_{az} c_s}{\omega_a}\right)^2\frac{m_i}{m_e} + \frac{\cos\alpha\,\sin\alpha}{\cos\beta(1-\sin^2\alpha)}\,\frac{k_a c_s}{\omega_a}\,\frac{k_{az} c_s}{\omega_a}\right\}, \tag{18}$$

where

$$C = \text{CONSTFACT}\,\frac{E_a E_b E_n^* \epsilon_o \omega_{pi}}{k_a k_b k_n c_s^4}\,\frac{q}{m_i}.$$

In both cases the first part of the expression is of order δ^2 and the second of δ^3. But the second term in M_{ion} is multiplied by a large numerical factor (10) and so the ratio of the two terms in M_{ion} is

```
(C9) BATCH([APIA,ION,DSK,PLASMA],ON);

(C9) (DOALL:TRUE,EZCFFSWITCH:TRUE,TIME:TRUE,KEEPFLOAT:FALSE,FLOAT:FALSE,DOTNONASSOC:TRUE,NOLABELS:TRUE)$
TIME= 22 MSEC.

(C10) RATVARS(KNZ[A],KNN[A],WN[B],WN[N],WN[A],LM4,LM3,LM2,LM1,%I,MU,DEL)$
TIME= 117 MSEC.
```

Here we put in the information about large and small parameters, expressing all in terms of DEL.

```
(C11) (KNX[A]:DEL*WN[A]*LM1,KNY[A]:0,KNZ[A]:KNX[A]*LM2*DEL,MU:1/DEL^2,WN[CI]:LM3*DEL*WN[A],WN[CE]:WN[A]/DEL^2/LM4)$
TIME= 183 MSEC.
```

Define two functions TAY and MATTAY. TAY(X,P) returns a Taylor series of X in DEL about 0 truncating at P. MATTAY does the same, but operates on a matrix, and returns a matrix each element of which is a Taylor series.

```
(C12) (TAY(X,P):=TAYLOR(EV(X),DEL,0,P),MATTAY(M,P):=MATRIXMAP(LAMBDA([V],TAY(V,P)),M))$
TIME= 27 MSEC.
```

Load in and display general expressions for ion terms of the coupling coefficient.

```
(C13) LOADFILE(SYMCC,ION,DSK,PLASMA)$

SYMCC ION DSK PLASMA BEING LOADED
LOADING DONE
TIME= 363 MSEC.

(C14) KN[I]:=[KNX[I],KNY[I],KNZ[I]]$
TIME= 65 MSEC.


(C15) DISPLAY(CONSTFACT,MICONV,MIFLOW,KN[A])$
```

$$\text{(E16)}\qquad \text{CONSTFACT} = \frac{E_A\, E_B\, E^*_N\, EP_O\, WN_{PI}^2\, Q}{KNM_A\, KNM_B\, W_{CI}\, MI_N\, KNM_S\, C}$$

$$\text{(E17)}\qquad \text{MICONV} = -\frac{(KN_A \,.\, VI_E)\,(VIT_N \,.\, VI_A) + (KN_B \,.\, VI_A)\,(VIT_N \,.\, VI_B)}{2\, WN_N}$$

$$\text{(E18)}\qquad \text{MIFLOW} = -\frac{NI_B\,(KN_N \,.\, VI_A) + NI_A\,(KN_N \,.\, VI_B)}{2\, WN_N}$$

$$\text{(E19)}\qquad KN_A = [WN_A\ \ LM1\ DEL,\ 0,\ WN_A\ \ LM1\ LM2\ DEL^2]$$

```
TIME= 19 MSEC.
```

Load in expression for SIGMAN applicable to a cold species, and use it as the basis of a functional definition of SIGMAN. With this definition when we reference a particular element of SIGMAN say SIGMAN[A], a Taylor series form applicable for mode A is returned.

```
(C20) LOADFILE(SIG,COLD,DSK,PLASMA)$

SIG COLD DSK PLASMA BEING LOADED
LOADING DONE
TIME= 551 MSEC.

(C21) (WN[C]:WN[CI],WN[P]:WN[PI])$
TIME= 23 MSEC.

(C22) SIG:MATRIXMAP(RATSIMP,SIGMAN[I])$
TIME= 3832 MSEC.

(C23) KILL(SIGMAN)$
TIME= 8 MSEC.

(C24) SIGMAN[K]:=MATRIXMAP(LAMBDA([V],TAYLOR(EV(V,I=K,EVAL),DEL,0,2)),SIG)$
TIME= 17 MSEC.
```

In the following command, the commands for the computation and display of VI, VIT and NI have been combined. Note that the truncation level has been adjusted to keep 3 significant terms in each expression. We have removed the truncation level from NI preparatory to calculating MICONV and MIFLOW. It is not necessary to do this with the velocities, since at the present time this is done automaticly prior to matrix multiplication.

```
(C25) BLOCK(DISPLAY(SIGMAN[A],SIGMAN[B],SIGMAN[N]),VI[A]:SIGMAN[A].KN[A],VI[A]:MATTAY(VI[A],3),DISPLAY(VI[A]),
VI[B]:SIGMAN[B].KN[B],VI[B]:MATTAY(VI[B],2),DISPLAY(VI[B]),NI[A]:(KN[A].VI[A])/WN[A],NI[A]:TAY(NI[A],4),
NI[A]:EV(NI[A]),DISPLAY(NI[A]),NI[B]:(KN[B].VI[B])/WN[B],NI[B]:TAY(NI[B],2),NI[B]:EV(NI[B]),DISPLAY(NI[B]),
VIT[N]:KN[N].SIGMAN[N],VIT[N]:MATTAY(VIT[N],2),DISPLAY(VIT[N]))$
```

$$\text{(E26)}\qquad \text{SIGMAN}_A = \begin{bmatrix} \frac{1}{WN_A} + \frac{LM3^2\, DEL^2}{WN_A} + \cdots & \frac{LM3\ \%I\ DEL}{WN_A} & 0 \\ -\frac{LM3\ \%I\ DEL}{WN_A} & \frac{1}{WN_A} + \frac{LM3^2\, DEL^2}{WN_A} + \cdots & 0 \\ 0 & 0 & \frac{1}{WN_A} \end{bmatrix}$$

Fig. VI-4. MACSYMA derivation of the ion terms of the coupling coefficient for coupling to ion acoustic waves.

(E27) $SIGMAN_B =$

$$\begin{bmatrix} \frac{1}{WN_B} + \frac{LM3^2\ WN_A^2\ DEL^2}{WN_B^3} + \cdots & \frac{LM3\ WN_A\ \%I\ DEL}{WN_B^2} & 0 \\ -\frac{LM3\ WN_A\ \%I\ DEL}{WN_B^2} & \frac{1}{WN_B} + \frac{LM3^2\ WN_A^2\ DEL^2}{WN_B^3} + \cdots & 0 \\ 0 & 0 & \frac{1}{WN_B} \end{bmatrix}$$

(E26) $SIGMAN_N =$

$$\begin{bmatrix} \frac{1}{WN_N} + \frac{LM3^2\ WN_A^2\ DEL^2}{WN_N^3} + \cdots & \frac{LM3\ WN_A\ \%I\ DEL}{WN_N^2} & 0 \\ -\frac{LM3\ WN_A\ \%I\ DEL}{WN_N^2} & \frac{1}{WN_N} + \frac{LM3^2\ WN_A^2\ DEL^2}{WN_N^3} + \cdots & 0 \\ 0 & 0 & \frac{1}{WN_N} \end{bmatrix}$$

(ROW TO COL CONVERSION MADE)

(E29) $VI_A =$

$$\begin{bmatrix} LM1\ DEL + LM3^2\ LM1\ DEL^3 + \cdots \\ -LM3\ LM1\ \%I\ DEL^2 \\ LM2\ LM1\ DEL^2 \end{bmatrix}$$

(ROW TO COL CONVERSION MADE)

(E30) $VI_B =$

$$\begin{bmatrix} \frac{KNX_B}{WN_B} + \frac{LM3\ KNY_B\ WN_A\ \%I\ DEL}{WN_B^2} + \frac{LM3^2\ WN_A^2\ KNX_B\ DEL^2}{WN_B^3} + \cdots \\ \frac{KNY_B}{WN_B} - \frac{LM3\ KNX_B\ WN_A\ \%I\ DEL}{WN_B^2} + \frac{LM3^2\ WN_A^2\ KNY_B\ DEL^2}{WN_B^3} + \cdots \\ \frac{KNZ_B}{WN_B} \end{bmatrix}$$

(E31) $$NI_A = LM1^2\ DEL^2 + (LM3^2 + LM2^2)\ LM1^2\ DEL^4$$

(E32) $$NI_B = \frac{(KNX_B^2 + KNY_B^2 + KNZ_B^2)\ WN_B^2 + (KNX_B^2 + KNY_B^2)\ WN_A^2\ LM3^2\ DEL^2}{WN_B^4}$$

(MATRIX DISPLAYED AS LIST OF LISTS)

(E33) $VI1_N$

$$= [[\frac{KNX_N}{WN_N} - \frac{KNY_N\ LM3\ WN_A\ \%I\ DEL}{WN_N^2} + \frac{LM3^2\ WN_A^2\ KNX_N\ DEL^2}{WN_N^3} + \cdots,$$

$$\frac{KNY_N}{WN_N} + \frac{KNX_N\ LM3\ WN_A\ \%I\ DEL}{WN_N^2} + \frac{LM3^2\ WN_A^2\ KNY_N\ DEL^2}{WN_N^3} + \cdots, \frac{KNZ_N}{WN_N}]]$$

TIME= 22975 MSEC.

Fig. VI-4. (continued).

```
(C34) KILL(SIGMAN,SIG)$
TIME= 16 MSEC.

Evaluate MICONV and MIFLOW and expand the result in a truncated Taylor series, the results being displayed term by
term.  Note that again we have chosen the truncation level to keep 3 significant terms.

(C35) MICONV:EV(MICONV,EVAL)$
TIME= 13095 MSEC.

(C36) MIFLOW:EV(MIFLOW,EVAL)$
TIME= 9041 MSEC.

(C37) KILL(ARRAYS,MU,MATTAY)$
TIME= 62 MSEC.

(C38) MICONV:TAY(MICONV,3)$
TIME= 63212 MSEC.

(C39) MIFLOW:TAY(MIFLOW,3)$
TIME= 12322 MSEC.

(C40) DISPTERMS(MICONV)$

+
```

$$\frac{(KNX_E^2\ LM1\ KNX_N + KNX_E\ LM1\ (KNY_B\ KNY_N + KNZ_B\ KNZ_N))\ DEL}{2\ WN_B\ WN_N^2}$$

$$-\ ((WN_B\ (KNX_B\ (-WN_A\ LM1^2\ KNX_N - KNZ_E\ LM1\ LM2\ KNX_N) + LM1\ (-KNY_B\ KNZ_B\ LM2\ KNY_N - KNZ_B^2\ LM2\ KNZ_N))\ WN_N$$

$$+ \%I\ (WN_B\ (-WN_A\ KNX_B\ KNY_E\ LM1\ LM3\ KNX_N + WN_A\ KNX_B^2\ LM1\ LM3\ KNY_N)$$

$$+ (-WN_A\ KNX_E\ KNY_B\ LM1\ LM3\ KNX_N + WN_A\ KNX_B^2\ LM1\ LM3\ KNY_N$$

$$+ WN_B\ (KNX_B\ KNY_B\ LM1\ LM3\ KNX_N + LM1\ (KNY_B^2\ LM3\ KNY_N + KNY_E\ KNZ_B\ LM3\ KNZ_N))\ WN_N)\ DEL^2)/(2\ WN_B^2\ WN_N^3)$$

$$-\ ((WN_E^2\ (WN_A^2\ KNX_B^2\ LM1\ LM3^2\ KNX_N + WN_A^2\ KNX_B\ KNY_E\ LM1\ LM3^2\ KNY_N)$$

$$- WN_B^2\ (-WN_A\ KNY_E^2\ LM1\ LM3^2\ KNX_N + WN_A\ KNX_B\ KNY_E\ LM1\ LM3^2\ KNY_N)\ WN_N$$

$$+ WN_B\ (WN_A^2\ KNX_B^2\ LM1\ LM3^2\ KNX_N + WN_A^2\ KNX_B\ KNY_B\ LM1\ LM3^2\ KNY_N)\ WN_N$$

$$- WN_B\ (-WN_A\ KNY_B^2\ LM1\ LM3^2\ KNX_N + WN_A\ KNX_B\ KNY_B\ LM1\ LM3^2\ KNY_N)\ WN_N^2$$

$$+ (WN_A^2\ KNX_B^2\ LM1\ LM3^2\ KNX_N + WN_A^2\ KNX_B\ KNY_B\ LM1\ LM3^2\ KNY_N$$

$$+ WN_B^2$$

$$(WN_A\ KNZ_B\ LM1^2\ LM2\ KNX_N + KNX_B^2\ LM1\ LM3^2\ KNX_N + KNX_B\ (WN_A\ LM1^2\ LM2\ KNZ_N + LM1\ (KNY_B\ LM3^2\ KNY_N + KNZ_B\ LM3^2\ KNZ_N))))$$

$$WN_N^2$$

$$+ \%I$$

$$(WN_B^2\ (WN_A\ KNY_E\ KNZ_B\ LM1\ LM2\ LM3\ KNX_N + KNX_B\ (-WN_A^2\ LM1^2\ LM3\ KNY_N - WN_A\ KNZ_B\ LM1\ LM2\ LM3\ KNY_N))\ WN_N$$

$$+ (-WN_A\ KNX_B\ WN_B^2\ LM1^2\ LM3\ KNY_N$$

$$+ WN_B\ (WN_A^2\ KNY_B\ LM1^2\ LM3\ KNX_N + WN_A\ KNY_B\ KNZ_B\ LM1\ LM2\ LM3\ KNX_N - WN_A\ KNX_B\ KNZ_B\ LM1\ LM2\ LM3\ KNY_N))\ WN_N^2)\ DEL^3)$$

$$/(2\ WN_B^3\ WN_N^4)$$

```
TIME= 14397 MSEC.
```

Fig. VI-4. (continued).

(C41) DISPTERMS(MIFLOW)$

+

$$-\frac{(KNY_B^2\ LM1\ KNX_N + LM1\ (KNX_B^2\ KNX_N + KNZ_B^2\ KNX_N))\ DEL}{2\ WN_B^2\ WN_N}$$

$$((-KNY_B\ WN_B\ LM1^2\ KNY_N + \%I\ (KNY_B^2\ LM1\ LM3\ KNY_N + (KNX_B^2 + KNZ_B^2)\ LM1\ LM3\ KNY_N) - KNY_B^2\ LM1\ LM2\ KNZ_N$$

$$+ WN_B\ LM1^2\ (-KNX_B\ KNX_N - KNZ_B\ KNZ_N) + LM1\ LM2\ (-KNX_B^2\ KNZ_N - KNZ_B^2\ KNZ_N))\ DEL^2)/(2\ WN_B^2\ WN_N)$$

$$-((KNY_B^2\ WN_B^2\ LM1\ LM3^2\ KNX_N + WN_B^2\ LM1\ LM3^2\ (KNX_B^2\ KNX_N + KNZ_B^2\ KNX_N)$$

$$+ WN_A^2\ (KNX_B^2\ LM1\ LM3^2\ KNX_N + KNY_B^2\ LM1\ LM3^2\ KNX_N) + \%I\ WN_A\ (KNY_B\ WN_B^2\ LM1^2\ LM3\ KNX_N - KNX_B\ WN_B^2\ LM1^2\ LM3\ KNY_N))\ DEL^3)$$

$$/(2\ WN_B^4\ WN_N)$$

TIME= 4398 MSEC.

At this stage we could combine terms. However the leading term (in DEL) would contain a factor (WN[B]+WN[N]) which is itself of order DEL. (Remember that WN[B] < 0.) To illustrate this and also to reduce the number of parameters in the final answer, we load in expressions for WN and KN in terms of ALP and BET (see Fig. 3). These are Taylor series truncated at DEL^2.

(C42) LOADFILE(IARSCN,TAY,DSK,CFK)$

IARSCN TAY DSK CFK BEING LOADED
LOADING DONE
TIME= 1112 MSEC.

(C43) DISPLAY(WN[A],WN[N],WN[B],KN[A],KN[N],KN[B])$

(E44) $$WN_A = WN_A$$

(E45) $$WN_N = \frac{WN_A}{2} + \frac{WN_A\ LM1\ SIN(ALP)\ DEL}{2} + \ . \ . \ .$$

(E46) $$WN_B = -\frac{WN_A}{2} + \frac{WN_A\ LM1\ SIN(ALP)\ DEL}{2} + \ . \ . \ .$$

(E47) $$KN_A = [WN_A\ LM1\ DEL,\ 0,\ WN_A\ LM1\ LM2\ DEL^2]$$

(E48) KN_N

$$= [\frac{WN_A\ SIN(ALP)}{2} + \frac{(-COS(BET)\ COS(ALP)\ LM2\ WN_A + WN_A\ LM1)\ DEL}{2}$$

$$+ \frac{((-LM2^2\ WN_A - WN_A\ LM1^2)\ SIN(ALP) + WN_A\ LM1^2\ SIN^3(ALP))\ DEL^2}{4} + \ . \ . \ . \ ,$$

$$\frac{SIN(BET)\ COS(ALP)\ WN_A}{2} + \frac{(-1 + SIN^2(ALP))\ LM1^2\ SIN(BET)\ COS(ALP)\ WN_A\ DEL^2}{4} + \ . \ . \ . \ ,$$

$$\frac{COS(BET)\ COS(ALP)\ WN_A}{2} + \frac{LM2\ WN_A\ SIN(ALP)\ DEL}{2}$$

$$+ ((-COS(BET)\ COS(ALP)\ LM2^2\ WN_A + 2\ LM2\ WN_A\ LM1 - COS(BET)\ COS(ALP)\ WN_A\ LM1^2 + COS(BET)\ COS(ALP)\ WN_A\ LM1^2\ SIN^2(ALP))$$

$$DEL^2)/4 + \ . \ . \ . \ ]$$

Fig. VI-4. (continued).

(E49) KN_B

$$= [\frac{WN_A\,\mathrm{SIN(ALP)}}{2} - \frac{(\mathrm{COS(BET)\,COS(ALP)}\,LM2\,WN_A + WN_A\,LM1)\,DEL}{2} + \frac{((-LM2^2\,WN_A - WN_A\,LM1^2)\,\mathrm{SIN(ALP)} + WN_A\,LM1^2\,\mathrm{SIN}^3(\mathrm{ALP}))\,DEL^2}{4} + \ldots,$$

$$\frac{\mathrm{SIN(BET)\,COS(ALP)}\,WN_A}{2} + \frac{(-1 + \mathrm{SIN}^2(\mathrm{ALP}))\,LM1^2\,\mathrm{SIN(BET)\,COS(ALP)}\,WN_A\,DEL^2}{4} + \ldots,$$

$$\frac{\mathrm{COS(BET)\,COS(ALP)}\,WN_A}{2} + \frac{LM2\,WN_A\,\mathrm{SIN(ALP)}\,DEL}{2}$$

$$+ ((-\mathrm{COS(BET)\,COS(ALP)}\,LM2^2\,WN_A - 2\,LM2\,WN_A\,LM1 - \mathrm{COS(BET)\,COS(ALP)}\,WN_A\,LM1^2 + \mathrm{COS(BET)\,COS(ALP)}\,WN_A\,LM1^2\,\mathrm{SIN}^2(\mathrm{ALP}))$$

$$DEL^2)/4 + \ldots]$$

TIME= 124 MSEC.

Since we wish to keep terms up to DEL^3 in the final answer we must reset the truncation level for WN and KN to 3. In C51 we define a function TRIGRED which effects some trigonometric identities.

```
(C50) BLOCK(KNX[B]:TAY(KNX[B],3),KNX[N]:TAY(KNX[N],3),KNY[B]:TAY(KNY[B],3),KNY[N]:TAY(KNY[N],3),
KNZ[B]:TAY(KNZ[B],3),KNZ[N]:TAY(KNZ[N],3),WN[B]:TAY(WN[B],3),WN[N]:TAY(WN[N],3))$
TIME= 8496 MSEC.

(C51) (TRIGRED(X):=SUBST([COS(ALP)^2=1-SIN(ALP)^2,COS(ALP)^3=COS(ALP)*(1-SIN(ALP)^2),COS(ALP)^4=(1-SIN(ALP)^2)^2,
COS(BET)^2=1-SIN(BET)^2,COS(BET)^3=COS(BET)*(1-SIN(BET)^2),COS(BET)^4=(1-SIN(BET)^2)^2],X),
KN[I]:=[KNX[I],KNY[I],KNZ[I]])$
TIME= 285 MSEC.
```

Evaluate MICONV and MIFLOW and combine them to obtain MION. Note that the leading terms have cancelled, so that it was necessary to keep 3 significant terms throughout the calculation in order to obtain 2 significant terms in the final answer.

```
(C52) MICONV:TRIGRED(EV(MICONV,EVAL));
TIME= 159176 MSEC.
```

(D52) $$-(-2\,\mathrm{SIN(ALP)}\,LM1\,DEL + ((2 - 2\,\mathrm{SIN}^2(\mathrm{ALP}))\,LM1^2 + 2\,\mathrm{COS(ALP)\,SIN(BET)}\,LM3\,LM1\,\%I)\,DEL^2$$

$$+ (((-2\,\mathrm{SIN(ALP)} - 8\,\mathrm{SIN}^3(\mathrm{ALP}) + (-8\,\mathrm{SIN(ALP)} + 8\,\mathrm{SIN}^3(\mathrm{ALP}))\,\mathrm{SIN}^2(\mathrm{BET}))\,LM3^2 - \mathrm{SIN(ALP)}\,LM2^2)\,LM1$$

$$+ (3\,\mathrm{SIN(ALP)} - 3\,\mathrm{SIN}^3(\mathrm{ALP}))\,LM1^3 + 18\,\mathrm{COS(ALP)\,SIN(ALP)\,SIN(BET)}\,LM3\,LM1^2\,\%I)\,DEL^3)/4$$

```
(C53) MIFLOW:TRIGRED(EV(MIFLOW,EVAL));
TIME= 89563 MSEC.
```

(D53) $$-(2\,\mathrm{SIN(ALP)}\,LM1\,DEL + (-2\,\mathrm{SIN}^2(\mathrm{ALP})\,LM1^2 - 2\,\mathrm{COS(ALP)\,SIN(BET)}\,LM3\,LM1\,\%I)\,DEL^2$$

$$+ (((2\,\mathrm{SIN(ALP)} + 8\,\mathrm{SIN}^3(\mathrm{ALP}) + (8\,\mathrm{SIN(ALP)} - 8\,\mathrm{SIN}^3(\mathrm{ALP}))\,\mathrm{SIN}^2(\mathrm{BET}))\,LM3^2 + \mathrm{SIN(ALP)}\,LM2^2)\,LM1$$

$$+ (-3\,\mathrm{SIN(ALP)} + 3\,\mathrm{SIN}^3(\mathrm{ALP}))\,LM1^3 + 2\,\mathrm{COS(ALP)\,SIN(ALP)\,SIN(BET)}\,LM3\,LM1^2\,\%I)\,DEL^3)/4$$

```
(C54) MION:MIFLOW+MICONV;
TIME= 175 MSEC.
```

(D54) $$-\frac{(1 - 2\,\mathrm{SIN}^2(\mathrm{ALP}))\,LM1^2\,DEL^2 + 10\,\mathrm{COS(ALP)\,SIN(ALP)\,SIN(BET)}\,LM3\,LM1^2\,\%I\,DEL^3}{2}$$

```
(C55) KILL(ARRAYS)$
TIME= 32 MSEC.
```

Finally we substitute for the LM's and multiply by CONSTFACT.

```
(C56) (DEL:1/SQRT(MU),LM1:KNM[A]*SQRT(MU)/WN[A],LM2:KNZ[A]/KNM[A]*SQRT(MU),LM3:SQRT(MU)/WN[A],LM4:WN[A])$
TIME= 147 MSEC.

(C57) MION:EV(TBOX(CONSTFACT)*TBOX(MION),EVAL);
TIME= 1623 MSEC.
```

(D57) $$\left(-\frac{(1 - 2\,\mathrm{SIN}^2(\mathrm{ALP}))\,KNM_A^2\,WN_A + 10\,\mathrm{COS(ALP)\,SIN(ALP)\,SIN(BET)}\,KNM_A^2\,\%I}{2\,WN_A^3}\right)\left(\frac{E_A\,E_B\,E*_N\,EP_O\,WN_{PI}^2\,Q}{KNM_A\,KNM_B\,W_{CI}\,MI\,KNM_N\,C_S}\right)$$

TIME= 474968 MSEC.

(D58) BATCH DONE

Fig. VI-4. (concluded).

$$10\,\frac{\Omega_i}{\omega_a}\,\frac{i\cos\alpha\,\sin\alpha\,\sin\beta}{1-2\,\sin^2\alpha}$$

which is of order 1 (if we ignore special angles), since $\Omega_i/\omega_a \sim 0.1$, and so in general we should keep both terms. Note that the first term was derived previously, under the assumption that the ions are magnetized,[1] so the second term is the finite magnetic field term arising from the ellipticity of the ion orbits, and in order to maximize this term we should try to make β as large as possible.

The ratio of terms in M_{el} (Eq. 18) (with the trigonometric factors ignored) is $k_a/k_{az}\mu$, which is only greater than unity if $\cos\theta < 1/\mu$, but in that case the whole electron term is small and so we are safe in discarding the second term in M_{el} to obtain

$$M_{el} = -C\left(\frac{k_{az}c_s}{a}\right)^2\mu. \tag{19}$$

This contribution comes from the electron pressure.

Comparing M_{el} and M_{ion}, we find

$$\frac{M_{el}}{M_{ion}} \approx \frac{k_{az}^2}{k_a} = \mu\cos^2\theta_a. \tag{20}$$

In choosing ω_a we were forced to take $\omega_a \approx \omega_{pi}$ in order to be able to couple to 2 ion acoustic modes. If the pump is a mode, we can only achieve that if

$$\cos^2\theta_a \ll \frac{1}{\mu}, \tag{21}$$

in which case we can neglect the electron contribution. But if we do not restrict ourselves to the pump being a mode, then Eq. 21 does not apply and, depending on the value of $\cos\theta_a$ that we have chosen, we may have to take $M = M_{ion}$, or $M_{ion} + M_{el}$, or M_{el}, with M_{ion} and M_{el} given by Eqs. 17 and 19, respectively.

Coupling to a Lower Hybrid Wave and a Low-Frequency Wave

In this case we take both the pump and idler (modes a and b) to be lower hybrid waves, which couple to some low-frequency wave (n). For the lower hybrid waves we may write $\omega^2 = \omega_{pi}^2(1+\mu\cos^2\theta)$; we take mode n to be either magnetosonic $\left(\omega^2 = k_z^2c_s^2\right)$ or electrostatic ion cyclotron $\left(\omega^2 = k^2c_s^2\left(\omega^2-\cos^2\theta\Omega_i^2\right)/\left(\omega^2-\Omega_i^2\right)\right)$. A typical case is shown in Fig. VI-5. Note that we take $k_{ay} = 0$ as before.

An expression for the coupling coefficient has been derived.[1]

$$M = C\left\{\frac{i}{2}\,\frac{k_{ax}c_s k_{by}c_s}{\omega_a \Omega_i} - \frac{1}{2}\,\frac{k_{az}c_s}{\omega_a}\,\frac{k_{bz}c_s}{\omega_b}\,\mu\right\}. \tag{22}$$

The source of these terms is the electron convective term. The real part is derived to include only the z components of the velocities (infinite magnetic field limit), and the imaginary part is the magnetic field correction resulting from $E \times B_o$ velocities in modes a and b.

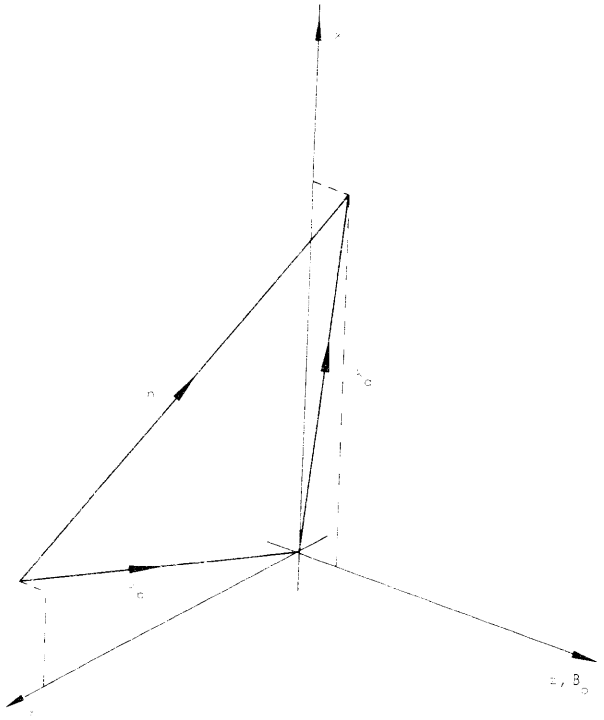

Fig. VI-5. Typical $\bar{k}$ space diagram for the case of a pump (a) and idler (b) above the lower hybrid frequency coupling to a low-frequency mode (n).

Using a simple form of ordering, $k_z \sim k\delta$ and $\omega \sim kc_s/\delta$ for modes a and b, we have found expressions for M in which the terms in Eq. 22 could be identified. The ordering that was chosen, however, was not good enough to separate these dominant terms from the others. In other words, the coefficients of the resulting polynomial in δ are themselves of order δ or $1/\delta$ or greater.

We are, therefore, investigating other finer ordering schemes. Since in such a case the order of the polynomial in the new small parameter δ is likely to be high, we may need a more efficient ordering and truncating function than TAYLOR. Most of the

expressions with which we deal are polynomials or ratios of polynomials; so instead of using TAYLOR which works on quite general expressions, we can use the MACSYMA function WEIGHT. With this function we assign weights to any number of variables; then if an expression that is a sum of products is put in a special rational form in MACSYMA, a term in the sum will be dropped if its combined weight (the sum of the weights of the terms of the product) exceeds a user set variable WTLEVEL. Examples of the use of these capabilities, and their application to the present problem, will be presented in a future report.

References

1. C. F. F. Karney, A. Bers, and J. L. Kulp, Quarterly Progress Report No. 110, Research Laboratory of Electronics, M. I. T., July 15, 1973, pp. 104-117.
2. A. Bers, J. L. Kulp, and D. C. Watson, Quarterly Progress Report No. 108, Research Laboratory of Electronics, M. I. T., January 15, 1973, pp. 167-185.
3. A. Bers, Notes on Lectures: Linear Waves and Instabilities, given at Ecole d'Eté de Physique Théorique, Les Houches, France, July 1972 (Gordon and Breach, New York, in press).

2. THIRD-ORDER NONLINEAR THEORY OF WAVE-WAVE INTERACTIONS

National Science Foundation (Grant GK-37979X)

D. C. Watson, A. Bers

Introduction

We present a theory of coherent wave coupling in the presence of a strong pump with arbitrary wave vector. With this theory we give a unified description of the modified parametric,[1] the nonoscillatory,[2] and the modified nonoscillatory[3] instabilities. The theory naturally admits a study of pump depletion and the effects of pump evolution.

Linear Behavior of Small Perturbations in the Presence of a Strong Pump

Consider a homogeneous medium with nonlinear conductivities to all orders. Let the medium sustain a pump-wave E field that is finite and of the form

$$\underline{E}_{pump}(\underline{x},t) = \underline{E}_o\, e^{i\underline{k}_o\cdot\underline{x} - i\omega_o t} + \underline{E}_o^*\, e^{-i\underline{k}_o\cdot\underline{x} + i\omega_o t}, \tag{1}$$

where the spatiotemporal frequency $(\underline{k}_o, \omega_o)$ is real. Then any small perturbing E field at any frequency $(\underline{k}, \omega)$ gives rise to nonlinear currents that are linear in this perturbing E field at all frequencies $(\underline{k} + n\underline{k}_o, \omega + n\omega_o)$. Thus, even the linear theory of small perturbations in the presence of the pump demands that we consider a set of such small

perturbations $\{\underline{E}_{(n)}\}$ separated by multiples of the pump frequency. The frequencies of this set may be denoted by

$$(\underline{k}_{(n)}, \omega_{(n)}) \equiv (\underline{k}_{(o)} + nk_o, \omega_{(o)} + n\omega_o). \tag{2}$$

For each small perturbation in the set Maxwell's equations give

$$\left\{\underline{k}_{(n)}\underline{k}_{(n)} - k^2_{(n)} + \left(\omega^2_{(n)}/c^2\right) + i\mu_o\omega_{(n)}\underline{\underline{\sigma}}^{\text{LINEAR}}\right\}\underline{E}_{(n)} = -i\mu_o\omega_{(n)}\left[\underline{J}^{NL(2)}_{(n)} + \underline{J}^{NL(3)}_{(n)} + \ldots\right], \tag{3}$$

where $\underline{J}^{NL(i)}_{(n)}$ is the i^{th}-order nonlinear current at the frequency $\omega_{(n)}$. Clearly a current that is 2^{nd}, 3^{rd}, ... order in electric field and only 1^{st} order in some perturbing field must be 1^{st}, 2^{nd}, ... order in the pump field. Thus the current at $(\underline{k}_{(n)}, \omega_{(n)})$ must arise from perturbation fields at frequencies accessible via one, two, ... frequency steps of magnitude $(\underline{k}_o, \omega_o)$. This observation enables us to write the right-hand side of (3) in terms of E fields.

$$\begin{aligned}
&\left\{\underline{k}_{(n)}\underline{k}_{(n)} - k^2_{(n)} + \left(\omega^2_{(n)}/c^2\right) + i\mu_o\omega_{(n)}\underline{\underline{\sigma}}^{\text{LINEAR}}_{(n)}\right\}\underline{E}_{(n)} \\
&= -i\mu_o\omega_{(n)}\Big[\underline{\underline{\sigma}}^{NL(2)}\underline{E}_{(n-1)}\underline{E}_o + \underline{\underline{\sigma}}^{NL(2)}\underline{E}_{(n+1)}\underline{E}^*_o \\
&\quad + (1/2!)\underline{\underline{\sigma}}^{NL(3)}\underline{E}_{(n-2)}\underline{E}_o\underline{E}_o + (1/2!)\underline{\underline{\sigma}}^{NL(3)}\underline{E}_{(n+2)}\underline{E}^*_o\underline{E}^*_o + \underline{\underline{\sigma}}^{NL(3)}\underline{E}_{(n)}\underline{E}_o\underline{E}^*_o + \ldots\Big].
\end{aligned} \tag{4}$$

For simplicity, the dependence of the nonlinear conductivities on frequency and wave vector has been suppressed. Equation 4 holds for each value of (n) and the resulting set of equations is linear in the set of perturbation fields $\{\underline{E}_{(n)}\}$. Thus the (infinite) matrix of coefficients of the components of these $\{\underline{E}_{(n)}\}$ must have a determinant equal to zero if a solution is to exist at the frequencies $\{(\underline{k}_{(n)}, \omega_{(n)})\}$.

If the polarizations of all $\{\underline{E}_{(n)}\}$ are known, then each $\underline{E}_{(n)}$ is specified completely by its scalar amplitude $u_{(n)}$. Here

$$\underline{E}_{(n)} = u_{(n)}\underline{e}_{(n)}$$

$$\underline{e}^*_{(n)} \cdot \underline{e}_{(n)} = 1.$$

The vector equation (4) may then be reduced to a scalar equation by taking its dot product with $\underline{e}^*_{(n)}$.

$$\left[\underline{e}^{*}_{(n)}\left\{\underline{k}_{(n)}\underline{k}_{(n)} \quad -k^{2}_{(n)}+(\omega^{2}_{(n)}/c^{2})+i\mu_{o}\omega_{(n)} \quad \underline{\underline{\sigma}}^{\text{LINEAR}}_{(n)}\right\}\underline{e}_{(n)}\right]u_{(n)}$$

$$= -i\mu_{o}\omega_{(n)}\left\{\left[\underline{e}^{*}_{(n)}\underline{\underline{\sigma}}^{\text{NL}(2)}\underline{e}_{(n-1)}\underline{e}_{o}u_{o}\right]u_{(n-1)}+\left[\underline{e}^{*}_{(n)}\underline{\underline{\sigma}}^{\text{NL}(2)}\underline{e}_{(n+1)}\underline{e}^{*}_{o}u^{*}_{o}\right]u_{(n+1)}\right.$$

$$+(1/2!)\left[\underline{e}^{*}_{(n)}\underline{\underline{\sigma}}^{\text{NL}(3)}\underline{e}_{(n-2)}\underline{e}_{o}\underline{e}_{o}u^{2}_{o}\right]u_{(n-2)}+(1/2!)\left[\underline{e}^{*}_{(n)}\underline{\underline{\sigma}}^{\text{NL}(3)}\underline{e}_{(n+2)}\underline{e}^{*}_{o}\underline{e}^{*}_{o}u^{*2}_{o}\right]u_{(n+2)}$$

$$\left.+\left[\underline{e}^{*}_{(n)}\underline{\underline{\sigma}}^{\text{NL}(3)}\underline{e}_{(n)}\underline{e}_{o}\underline{e}^{*}_{o}u_{o}u^{*}_{o}\right]u_{(n)}+\cdots\right\}. \tag{5}$$

This set of equations, linear in the set of scalar amplitudes $\{u_{(n)}\}$, is consistent if the (infinite) matrix of the coefficients of the $\{u_{(n)}\}$ has determinant zero. Divide (5) by $\omega^{2}_{(n)}/c^{2}$ and write it as

$$K_{(n)}u_{(n)} = -i\left\{\left[\frac{\underline{e}^{*}_{(n)}\cdot\underline{j}^{\text{NL}(2)}_{(n-1),\,o}}{\epsilon_{o}\omega_{(n)}}u_{o}\right]u_{(n-1)}+\left[\frac{\underline{e}^{*}_{(n)}\cdot\underline{j}^{\text{NL}(2)}_{(n+1),\,-o}}{\epsilon_{o}\omega_{(n)}}u^{*}_{o}\right]u_{(n+1)}\right.$$

$$+\frac{1}{2!}\left[\frac{\underline{e}^{*}_{(n)}\cdot\underline{j}^{\text{NL}(3)}_{(n-2),\,o,\,o}}{\epsilon_{o}\omega_{(n)}}u^{2}_{o}\right]u_{(n-2)}+\frac{1}{2!}\left[\frac{\underline{e}^{*}_{(n)}\cdot\underline{j}^{\text{NL}(2)}_{(n+2),\,-o,\,-o}}{\epsilon_{o}\omega_{(n)}}u^{*2}_{o}\right]u_{(n+2)}$$

$$\left.+\left[\frac{\underline{e}^{*}_{(n)}\cdot\underline{j}^{\text{NL}(3)}_{(n),\,o,\,-o}}{\epsilon_{o}\omega_{(n)}}u_{o}u^{*}_{o}\right]u_{(n)}+\cdots\right\}. \tag{6}$$

Here

$$K_{(n)} \equiv \underline{e}^{*}_{(n)}\left\{\frac{\underline{k}^{c}_{(n)}}{\omega_{(n)}}\frac{\underline{k}^{c}_{(n)}}{\omega_{(n)}}-\frac{k^{2}_{(n)}c^{2}}{\omega^{2}_{(n)}}+1+\frac{i\,\underline{\underline{\sigma}}^{\text{LINEAR}}_{(n)}}{\epsilon_{o}\omega_{(n)}}\right\}e_{(n)}$$

is essentially the dispersion relation for the linear perturbation in the absence of the pump. The square brackets on the right-hand side of (6) are essentially normalized coupling coefficients multiplied by pump amplitudes. The $\{K_{(n)}\}$ and the square brackets are coefficients of the $\{u_{(n)}\}$ and will therefore appear as entries in the matrix whose determinant is to be equated to zero. In case only 3 perturbations are considered this determinantal equation becomes finite and has the form

$$\begin{vmatrix} K_{(1)} + i\left[\dfrac{\underline{e}^*_{(1)} \cdot \underline{j}^{NL(3)}_{(1),o,-o}}{\epsilon_o \omega_{(1)}} u_o u_o^*\right] & i\left[\dfrac{\underline{e}^*_{(1)} \cdot \underline{j}^{NL(2)}_{(o),o}}{\epsilon_o \omega_{(1)}} u_o\right] & \dfrac{i}{2!}\left[\dfrac{\underline{e}^*_{(1)} \cdot \underline{j}^{NL(3)}_{(-1),o,o}}{\epsilon_o \omega_{(1)}} u_o^2\right] \\ i\left[\dfrac{\underline{e}^*_{(o)} \cdot \underline{j}^{NL(2)}_{(1),-o}}{\epsilon_o \omega_{(o)}} u_o^*\right] & K_{(o)} + i\left[\dfrac{\underline{e}^*_{(o)} \cdot \underline{j}^{NL(3)}_{(o),o,-o}}{\epsilon_o \omega_{(o)}} u_o u_o^*\right] & i\left[\dfrac{\underline{e}^*_{(o)} \cdot \underline{j}^{NL(2)}_{(-1),o}}{\epsilon_o \omega_{(o)}} u_o\right] \\ \dfrac{i}{2!}\left[\dfrac{\underline{e}^*_{(-1)} \cdot \underline{j}^{NL(3)}_{(1),-o,-o}}{\epsilon_o \omega_{(-1)}} u_o^{*2}\right] & i\left[\dfrac{\underline{e}^*_{(-1)} \cdot \underline{j}^{NL(2)}_{(o),-o}}{\epsilon_o \omega_{(-1)}} u_o^*\right] & K_{(-1)} + i\left[\dfrac{\underline{e}^*_{(-1)} \cdot \underline{j}^{NL(3)}_{(-1),o,-o}}{\epsilon_o \omega_{(-1)}} u_o u_o^*\right] \end{vmatrix} = 0 \tag{7}$$

Assume an electromagnetic pump near the plasma frequency. Note that (7) has the following solutions when $|u_o| = 0$:

$$\begin{aligned} &K^{EM}_{(1)} = 0, \quad (\underline{k}_{(o)}, \omega_{(o)}) = (\underline{k}_{(1)}, \omega_{EM}(k_{(1)})) - (\underline{k}_o, \omega_o) \\ &K^{ES}_{(1)} = 0, \quad (\underline{k}_{(o)}, \omega_{(o)}) = (\underline{k}_{(1)}, \omega_{BG}(k_{(1)})) - (\underline{k}_o, \omega_o) \\ &K^{ES}_{(o)} = 0, \quad (\underline{k}_{(o)}, \omega_{(o)}) = (\underline{k}_{(o)}, \omega_{IA}(k_{(o)})) \\ &K^{ES}_{(-1)} = 0, \quad (\underline{k}_{(o)}, \omega_{(o)}) = (\underline{k}_{(-1)}, -\omega_{BG}(k_{(-1)})) + (\underline{k}_o, \omega_o) \\ &K^{EM}_{(-1)} = 0, \quad (\underline{k}_{(o)}, \omega_{(o)}) = (\underline{k}_{(-1)}, -\omega_{EM}(k_{(-1)})) + (\underline{k}_o, \omega_o). \end{aligned} \tag{8}$$

Now take the z axis along $\underline{k}_o$ and graph the solutions (8) in the ω-$k_{(o)z}$ plane for various values of $k_{(o)x}$, $k_{(o)y}$. It is simpler to draw the graph first for the values $k_{(o)x} = k_{(o)y} = 0$. The possible loci for $(k_{(o)z}, \omega_{(o)})$ are then: positive HF (electromagnetic and Bohm-Gross) dispersion curves with the pump spatiotemporal frequency subtracted, negative HF (electromagnetic and Bohm-Gross) dispersion curves with the pump spatiotemporal frequency added, and the LF (ion-acoustic) dispersion curve.

The labeled points in Fig. VI-6 are intersections of dispersion curves with opposite gradients. From the usual coupling-of-modes theory we predict the possibility of corresponding instabilities for $|u_o| \neq 0$. Indeed A, A' indicate the possibility of coupling together an electron-plasma wave and an ion-acoustic wave by means of the pump acting once. Thus A, A' correspond to decay instabilities. B indicates the possibility of coupling together two opposite-going plasma waves by means of the pump acting twice. In the approximation $k_o = 0$, the point B falls on the k axis and the corresponding instability is called the "nonoscillatory instability." C indicates the possibility of coupling together an electromagnetic wave and an ion-acoustic wave by means of the pump acting once, and corresponds to the stimulated Brillouin scattering. D indicates the possibility of coupling

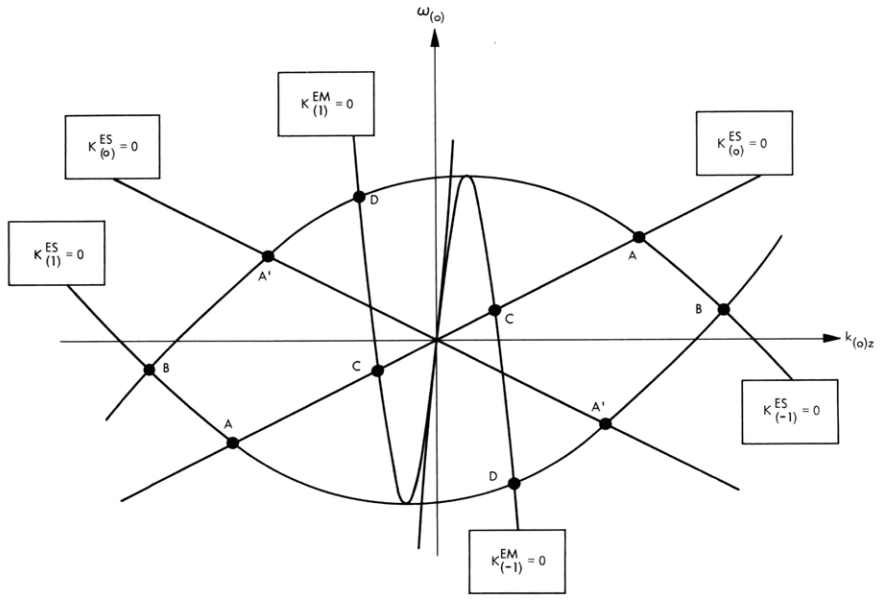

Fig. VI-6. Possible loci for $(\omega_{(o)}, k_{(o)z})$ when $k_{(o)\perp} = 0$.

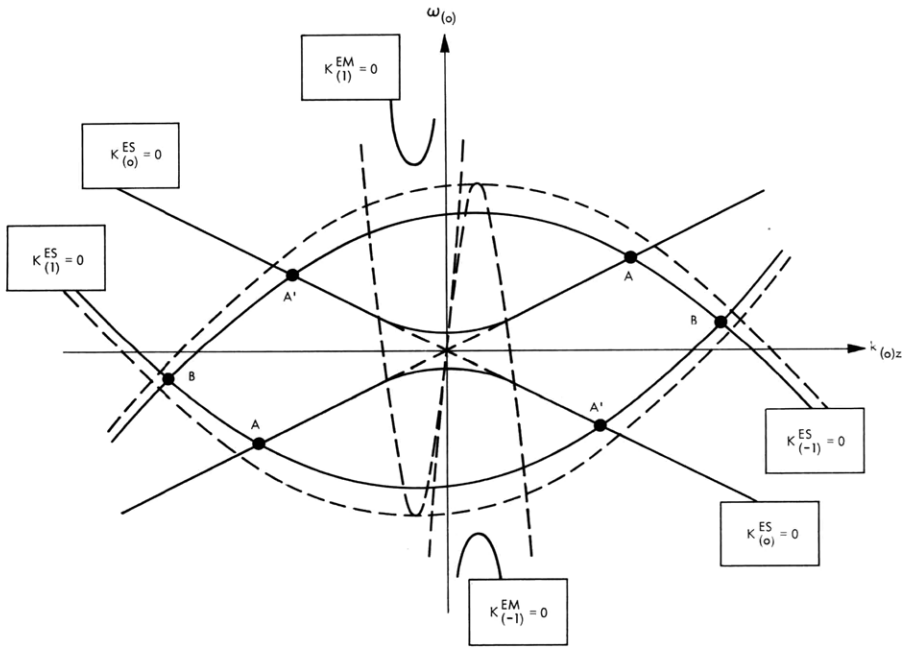

Fig. VI-7. Possible loci for $(\omega_{(o)}, k_{(o)z})$ when $k_{(o)\perp} \neq 0$.

together a plasma wave and an opposite-going electromagnetic wave by means of the pump acting twice. This may be termed the 3rd-order hybrid instability. Since A, A', B correspond to purely electrostatic perturbations, they cannot be driven unstable by a transversely polarized pump unless $\underline{k}_{(o)}$ is given a nonzero part

$$k_{(o)\perp} = \sqrt{k_{(o)x}^2 + k_{(o)y}^2}$$

in the transverse direction.

With the same pump wave as before, draw the graph of (8) for $k_{(o)\perp} \neq 0$. The functions $\omega_{EM}(k_{(1)z})$, $\omega_{BG}(k_{(1)z})$, $\omega_{IA}(k_{(o)z})$, $-\omega_{BG}(k_{(-1)z})$, $-\omega_{EM}(k_{(-1)z})$ are now replaced by the functions $\omega_{EM}\left(\sqrt{k_{(o)\perp}^2 + k_{(1)z}^2}\right)$, $\omega_{BG}\left(\sqrt{k_{(o)\perp}^2 + k_{(1)z}^2}\right)$, $\omega_{IA}\left(\sqrt{k_{(o)\perp}^2 + k_{(o)z}^2}\right)$, $-\omega_{BG}\left(\sqrt{k_{(o)\perp}^2 + k_{(-1)z}^2}\right)$, $-\omega_{EM}\left(\sqrt{k_{(o)\perp}^2 + k_{(-1)z}^2}\right)$.

The lowering and raising of the resulting curves to form possible loci for $(k_{(o)z}, \omega_{(o)})$ goes through as before. The graph of (8) then looks as shown in Fig. VI-7.

Compared with Fig. VI-6, the curves for $K_{(\pm 1)}^{EM} = 0$ are roughly displaced upward and downward, respectively, by $k_{(o)\perp}^2 c^2/2\omega_p$. The curves for $K_{(\pm 1)}^{ES} = 0$ are roughly displaced upward and downward, respectively, by $3k_{(o)\perp}^2 v_{Te}^2/2\omega_p$. The two halves of the curve for $K_{(o)}^{ES} = 0$ are displaced at the center, upward and downward respectively, by $k_{(o)\perp} c_S$.

Evaluation of the Normalized Coupling Coefficients

Specialize to a driftless unmagnetized plasma and use the two-warm-fluids model. A wave specified by $\underline{e}_a$, $\underline{k}_a$, ω_a then induces a first-order velocity and density for each species given by

$$\begin{aligned} \underline{v}_a &= i\underline{\underline{M}}_a \frac{q\underline{e}_a}{m\omega_a}, \\ \frac{n_a}{n_E} &= \frac{\underline{k}_a \cdot \underline{v}_a}{\omega_a}, \end{aligned} \tag{9}$$

where n_E is the unperturbed particle density, and

$$\underline{\underline{M}}_a^{-1} = 1 - \frac{\underline{k}_a \underline{k}_a \gamma v_T^2}{\omega_a^2}.$$

Two waves specified by $\underline{e}_a, \underline{k}_a, \omega_a$ and $\underline{e}_b, \underline{k}_b, \omega_b$, respectively, induce a second-order

velocity and density for each species given by

$$\underline{v}_{a+b} = \underline{\underline{M}}_{a+b} \frac{\underline{k}_{a+b}}{\omega_{a+b}} \left[\underline{v}_a \cdot \underline{v}_b + \gamma v_T^2 \frac{\underline{k}_{a+b}}{\omega_{a+b}} \cdot \left(\underline{v}_a \frac{n_b}{n_E} + \underline{v}_b \frac{n_a}{n_E} \right) + \gamma(\gamma-2)\, v_T^2 \frac{n_a n_b}{n_E^2} \right]$$

$$n_{a+b} = \frac{\underline{k}_{a+b}}{\omega_{a+b}} \cdot \left[\underline{v}_{a+b} + \underline{v}_a \frac{n_b}{n_E} + \underline{v}_b \frac{n_a}{n_E} \right]. \tag{10}$$

The normalized coupling coefficients in (7) are conveniently displayed in terms of these induced velocities and densities as follows:

$$\frac{\underline{e}_a^* \cdot \underline{j}_{b,c}^{NL(2)}}{\epsilon_o \omega_a} = \sum_{\text{species}} \frac{im}{\epsilon_o} \sum_{\substack{6 \text{ permutations} \\ \text{of } (-a, b, c)}} \left\{ \frac{1}{2} n_{-a} (\underline{v}_b \cdot \underline{v}_c) + \frac{1}{6} \frac{n_{-a} n_b n_c}{n_E^2} \gamma(\gamma-2)\, v_T^2 \right\}. \tag{11}$$

$$\frac{\underline{e}_a^* \cdot \underline{j}_{b,c,d}^{NL(3)}}{\epsilon_o \omega_a} = \sum_{\text{species}} \frac{im}{\epsilon_o} \sum_{\substack{24 \text{ permutations} \\ \text{of } (-a, b, c, d)}} \left\{ \frac{1}{2} n_{-a} \underline{v}_{b+c} \cdot \underline{v}_d + \frac{1}{8} n_E \underline{v}_{-a+b} \cdot \underline{v}_{c+d} - \frac{1}{8} \frac{n_{-a+b} n_{c+d}}{n_E} \gamma v_T^2 + \frac{1}{24} \frac{n_{-a} n_b n_c n_d}{n_E^3} \gamma(\gamma-2)(\gamma-3)\, v_T^2 \right\}. \tag{12}$$

Here the subscript $-a$ is used to denote quantities calculated by using (9) and (10) with $(\underline{k}_a, \omega_a)$ replaced by $(-\underline{k}_a, -\omega_a)$.

Coupling Coefficients for an Electromagnetic Pump near the Plasma Frequency

Now introduce approximations based on this physical situation. Take $\omega_{(1)}$ and ω_o to be near the plasma frequency ω_p. Take $\omega_{(-1)}$ to lie near $-\omega_p$. Take $|\omega_{(o)}|$ to be much smaller than ω_p. The physical picture is of a pump whose frequency is roughly around the plasma frequency, coupling together a triplet of perturbations; an HF perturbation, an LF perturbation, and a negative HF perturbation. Ignore the perturbations at $\omega_{(\pm 2)} \approx \pm 2\omega_p$ at which frequencies the plasma response is minimal. Then the infinite matrix of coefficients of the $\{u_{(n)}\}$ reduces to the 3×3 matrix of the coefficients of $\{u_{(1)}, u_{(o)}, u_{(-1)}\}$ displayed in (7).

Furthermore, take the phase velocities of the pump and the positive and negative HF perturbations to be much greater than the electron thermal velocity, but take the phase velocity of the LF perturbation to be much less than the electron thermal velocity

$$\frac{|\omega_o|}{|k_o|}, \quad \frac{|\omega_{(1)}|}{|k_{(1)}|}, \text{ d } \frac{|\omega_{(-1)}|}{|k_{(-1)}|} \gg v_{Te} \gg \frac{|\omega_{(o)}|}{|k_{(o)}|}.$$

Note that within this approximation we cannot consider interactions C and D in Fig. VI-6. These will be treated separately. Assume the LF phase velocity is not near the ion thermal velocity. Then the ion contribution to the second-order coupling coefficients is smaller than the electron contribution by a factor of order $(m_e/m_i)(T_e/T_i)$, and the ion contribution to the third-order coupling coefficients is smaller than the electron contribution by a factor of order $(m_e/m_i)^2 (T_e/T_i)$. The electron contributions may be evaluated rapidly by using these approximations. Without loss of generality, define the pump amplitude u_o to be real and positive and define $\Lambda \equiv eu_o/m_e\lambda_{De}\omega_o^2$. The quantity Λ is a measure of the pump strength:

$$\Lambda = \frac{\text{peak electron excursion induced by the pump}}{2(\text{electron Debye length})}.$$

To within the approximation introduced above,

$$\Lambda \approx \frac{\text{peak electron velocity induced by the pump}}{2(\text{electron thermal velocity})}.$$

Then the coupling coefficients as represented by their electron contributions (take $\gamma = 1$ for coupling to a low phase-velocity mode) are

$$\frac{\underline{e}^*_{(1)} \cdot \underline{j}^{NL(2)}_{(o),\,o}}{\epsilon_o \omega_{(1)}} u_o \cong -\frac{\Lambda}{k_{(o)}\lambda_{De}} \mu_S^*$$

$$\frac{\underline{e}^*_{(-1)} \cdot \underline{j}^{NL(2)}_{(o),\,-o}}{\epsilon_o \omega_{(-1)}} u_o^* \cong -\frac{\Lambda}{k_{(o)}\lambda_{De}} \mu_A^*$$

$$\frac{\underline{e}^*_{(o)} \cdot \underline{j}^{NL(2)}_{(1),\,-o}}{\epsilon_o \omega_{(o)}} u_o^* \cong \frac{\Lambda}{k_{(o)}\lambda_{De}} \mu_S$$

$$\frac{\underline{e}^*_{(o)} \cdot \underline{j}^{NL(2)}_{(-1),\,o}}{\epsilon_o \omega_{(o)}} u_o \cong \frac{\Lambda}{k_{(o)}\lambda_{De}} \mu_A$$

$$\frac{\underline{e}^*_{(1)} \cdot \underline{j}^{NL(3)}_{(-1),\,o,\,o}}{\epsilon_o \omega_{(1)}} u_o^2 \cong -2i\Lambda^2 \mu_S^* \mu_A$$

$$\frac{\underline{e}^*_{(-1)} \cdot \underline{j}^{NL(3)}_{(1),-o,-o}}{\epsilon_o \omega_{(-1)}} u_o^{*2} \cong -2i\Lambda^2 \mu_S \mu_A^*$$

$$\frac{\underline{e}^*_{(1)} \cdot \underline{j}^{NL(3)}_{(1),o,-o}}{\epsilon_o \omega_{(1)}} u_o u_o^* \cong -i\Lambda^2 |\mu_S|^2$$

$$\frac{\underline{e}^*_{(-1)} \cdot \underline{j}^{NL(3)}_{(-1),o,-o}}{\epsilon_o \omega_{(-1)}} u_o u_o^* \cong -i\Lambda^2 |\mu_A|^2$$

$$\frac{\underline{e}^*_{(o)} \cdot \underline{j}^{NL(3)}_{(o),o,-o}}{\epsilon_o \omega_{(o)}} u_o u_o^* \cong -i\mu_L \Lambda^2. \tag{13}$$

Here the μ are geometrical factors defined as follows.

$\mu_S = \underline{e}^*_o \cdot \underline{e}_{(1)}$ describes the relative alignment of the pump and positive HF perturbation polarizations;

$\mu_A = \underline{e}^*_o \cdot \underline{e}_{(-1)}$ describes the relative alignment of the pump and negative HF perturbations;

μ_L is a complicated geometrical factor that can be shown to be of order unity provided $\frac{\omega_{(o)}}{\omega_{pe}} < k^2_{(o)}\lambda^2_{De}$, and of order $\frac{\omega_{(o)}/\omega_{pe}}{k^2_{(o)}\lambda^2_{De}}$ in case $\frac{\omega_{(o)}}{\omega_{pe}} > k^2_{(o)}\lambda^2_{De}$. We substitute the results (13) in (7), and get

$$\begin{vmatrix} K_{(1)} + \Lambda^2 |\mu_S|^2 & -i(\Lambda/k_{(o)}\lambda_{De})\,\mu_S^* & \Lambda^2 \mu_S^* \mu_A \\ i(\Lambda/k_{(o)}\lambda_{De})\,\mu_S & K_{(o)} + \Lambda^2 \mu_L & i(\Lambda/k_{(o)}\lambda_{De})\,\mu_A \\ \Lambda^2 \mu_S \mu_A^* & -i(\Lambda/k_{(o)}\lambda_{De})\,\mu_A^* & K_{(-1)} + \Lambda^2 |\mu_A|^2 \end{vmatrix} = 0. \tag{14}$$

Multiplying the rows by $1/\mu_S^*$, $ik_{(o)}\lambda_{De}$, $1/\mu_A^*$ and the columns by $1/\mu_S$, $-ik_{(o)}\lambda_{De}$, $1/\mu_A$, respectively, we obtain

$$\begin{vmatrix} \left(K_{(1)}/|\mu_S|^2\right) + \Lambda^2 & \Lambda & \Lambda^2 \\ \Lambda & K_{(o)}k^2_{(o)}\lambda^2_{De} + \chi\Lambda^2 & \Lambda \\ \Lambda^2 & \Lambda & \left(K_{(-1)}/|\mu_A|^2\right) + \Lambda^2 \end{vmatrix} = 0, \tag{15}$$

where χ is of order $k_{(o)}^2\lambda_{De}^2$ or of order $\omega_{(o)}/\omega_{pe}$, whichever is larger. Expanding (15), we obtain

$$\frac{K_{(1)}}{|\mu_S|^2}\frac{K_{(-1)}}{|\mu_A|^2} = -\Lambda^2\left(\frac{K_{(1)}}{|\mu_S|^2}+\frac{K_{(-1)}}{|\mu_A|^2}\right)\left(\frac{K_{(o)}k_{(o)}^2\lambda_{De}^2-1+\chi\Lambda^2}{K_{(o)}k_{(o)}^2\lambda_{De}^2+\chi\Lambda^2}\right). \tag{16}$$

Note that for an electrostatic high-frequency (ESHF) perturbation

$$K_{(\pm1)} \cong 1-\frac{\omega_p^2}{\omega_{(\pm1)}^2-3k_{(\pm1)}^2v_{Te}^2}. \tag{17}$$

Note that for an electromagnetic high-frequency (EMHF) perturbation

$$K_{(\pm1)} \cong 1-\frac{\left(\omega_p^2+k^2c^2\right)}{\omega_{(\pm1)}^2}. \tag{18}$$

Note that for an electrostatic low-frequency (ESLF) perturbation

$$K_{(o)}k_{(o)}^2\lambda_{De}^2 \cong 1-\frac{k_{(o)}^2c_S^2}{\omega_{(o)}^2}. \tag{19}$$

a. Parametric Decay Instability

Let Λ be small but nonzero and examine the neighborhood of the intersection A for possible instability. Set $(k_{(o)z}, \omega_{(o)}) = (k_A, \omega_A+\Delta\omega)$, where $\Delta\omega$ and hence $K_{(1)}$, $K_{(o)}k_{(o)}^2\lambda_{De}^2$ are of order Λ. Then (16) reduces to

$$\frac{K_{(1)}}{|\mu_S|^2}K_{(o)}k_{(o)}^2\lambda_{De}^2 = \Lambda^2.$$

Now expand in Taylor's series about ω_A.

$$\left(\frac{2\Delta\omega}{\omega_p}\right)\left(\frac{-2\Delta\omega}{\omega_{IA}(k_A)}\right) = |\mu_S|^2\Lambda^2. \tag{20}$$

The root of (20) is $\Delta\omega = i\gamma$, where

$$\gamma^2 = \Lambda^2 |\mu_S|^2 \frac{\omega_p \omega_{IA}}{4}$$

$$\gamma^2 = \frac{V_o^2 \left(\underline{e}_o^* \cdot \underline{e}_{(1)}\right)^2 \omega_p \omega_{IA}}{16\, v_{Te}^2}.$$

This is the usual decay instability growth rate.

b. Modified Decay Instability

Assume that $K_{(1)} \ll K_{(-1)}$, then (16) reduces to

$$\frac{K_{(1)}}{|\mu_S|^2} = \Lambda^2 \left\{ \frac{1 - K_{(o)} k_{(o)}^2 \lambda_{De}^2 - \chi\Lambda^2}{K_{(o)} k_{(o)}^2 \lambda_{De}^2 + \chi\Lambda^2} \right\}. \tag{21}$$

This is the same as the 2×2 determinantal equation obtained by truncating (15):

$$\begin{vmatrix} \left(K_{(1)}/|\mu_S|^2\right) + \Lambda^2 & \Lambda \\ \Lambda & K_{(o)} k_{(o)}^2 \lambda_{De}^2 + \chi\Lambda^2 \end{vmatrix} = 0. \tag{22}$$

It describes the parametric coupling of modes which incorporates self-corrections to their dielectric constants that are due to the pump. Assume

$$|\chi\Lambda^2| \ll |K_{(o)} k_{(o)}^2 \lambda_{De}^2|$$

$$|\chi\Lambda^2| \ll |1 - K_{(o)} k_{(o)}^2 \lambda_{De}^2|$$

so that the LF self-correction is negligible, then (21) reduces to

$$\frac{K_{(1)}}{|\mu_S|^2} = \Lambda^2 \left(\frac{1 - K_{(o)} k_{(o)}^2 \lambda_{De}^2}{K_{(o)} k_{(o)}^2 \lambda_{De}^2} \right). \tag{23}$$

Assume finally that $\omega_{IA} \ll |\omega_{(o)}| \ll \omega_{pe}$ so that the LF dielectric function is strongly modified, whereas the HF dielectric function may be approximated by its Taylor's series expansion in ω about ω_A. Then (23) becomes

$$\frac{2\Delta\omega}{\omega_p} \approx \frac{2\omega_{(o)}}{\omega_p} = \Lambda^2 |\mu_S|^2 \left(\frac{\omega_{IA}^2}{\omega_{(o)}^2 - \omega_{IA}^2} \right) \approx \frac{\Lambda^2 |\mu_S|^2 \omega_{IA}^2}{\omega_{(o)}^2}$$

$$2\omega_{(o)}^3 = \Lambda^2 |\mu_S|^2 \omega_{IA}^2 \omega_p. \tag{24}$$

This has a root for which

$$\text{Im}(\omega_{(o)}) \equiv \gamma = \frac{3^{1/2}}{2^{4/3}} (\Lambda |\mu_S|)^{2/3} \left(\omega_{IA}^2 \omega_p\right)^{1/3}. \tag{25}$$

This is the modified decay instability growth rate. The assumptions $K_{(1)} \ll K_{(-1)}$ and $\omega_{IA} \ll |\omega_{(o)}|$ are consistent only if the intersection B lies at a point (k_B, ω_B) so that $(\omega_B/k_B c_S)$ is very large. This requires that the pump, while $\sim\omega_p$, satisfy $k_o \lambda_{De} \gg m_e/m_i$. For an electromagnetic pump, this is not trivial, but with an electrostatic pump wave this may be satisfied easily. The assumption $|\chi\Lambda^2| \ll |1 - K_{(o)} k_{(o)}^2 \lambda_{De}^2|$ is consistent with the result (24) only if

$$\omega_{(o)}^3 \ll \omega_{IA}^2 \omega_p$$

$$\Lambda^2 \ll 1.$$

This is consistent with the assumption $|\omega_{(o)}| \gg \omega_{IA}$ only if $1 \ll (\omega_p/\omega_{IA})^{1/3}$. If this is not satisfied, (24) must be replaced by (21), which results in a more complicated cubic equation for $\omega_{(o)}$.

c. "Nonoscillatory" Instability

Let Λ be small but nonzero and examine the neighborhood of B for possible instability. Note that B is not near the ion-acoustic dispersion curve so that $K_{(o)} k_{(o)}^2 \lambda_{De}^2$ is large and the term $\chi\Lambda^2$ may be neglected in (16); hence, (16) reduces to

$$\frac{K_{(1)}}{|\mu_S|^2} \frac{K_{(-1)}}{|\mu_A|^2} = -\Lambda^2 \left(\frac{K_{(1)}}{|\mu_S|^2} + \frac{K_{(-1)}}{|\mu_A|^2} \right) \left(\frac{K_{(o)} k_{(o)}^2 \lambda_{De}^2 - 1}{K_{(o)} k_{(o)}^2 \lambda_{De}^2} \right). \tag{26}$$

Set $(k_{(o)z}, \omega_{(o)}) = (k_B + \Delta k, \omega_B + \Delta\omega)$. Note that $K_{(1)}$, $K_{(-1)}$ are of the order of $(\Delta k, \Delta\omega)$ which must therefore be of order Λ^2. Make a Taylor's series expansion in k and ω of $K_{(1)}$ and $K_{(-1)}$, and approximate $K_{(o)} k_{(o)}^2 \lambda_{De}^2$ by a constant. Then (26) becomes

$$\frac{2\left(\Delta\omega - |v_g^{(1)}|\Delta k\right)}{\omega_p|\mu_S|^2}\ \frac{2\left(-\Delta\omega - |v_g^{(-1)}|\Delta k\right)}{\omega_p|\mu_A|^2} = -\Lambda^2\left(\frac{-2|v_g^{(1)}|}{|\mu_S|^2} - \frac{2|v_g^{(-1)}|}{|\mu_A|^2}\right)\frac{\Delta k}{\omega_p}\left(\frac{-k_B c_S^2}{\omega_B^2 - k_B^2 c_S^2}\right). \tag{27}$$

Take $|\underline{k}_o| \ll |\underline{k}_{(-1)}|, |k_{(1)}|$. Then $|\mu_S| \cong |\mu_A|$ and

$$4\left(\Delta\omega - |v_g^{(1)}|\Delta k\right)\left(\Delta\omega + |v_g^{(-1)}|\Delta k\right) = -\Lambda^2|\mu_S|^2\left(2|v_g^{(1)}| + 2|v_g^{(-1)}|\right)\Delta k\omega_p\ \frac{k_B^2 c_S^2}{k_B^2 c_S^2 - \omega_B^2}\ .$$

Set

$$|v_g^{(1)}| \equiv u_g + w_g$$

$$|v_g^{(-1)}| \equiv u_g - w_g$$

$$|\mu_S|^2\ \frac{k_B^2 c_S^2}{k_B^2 c_S^2 - \omega_B^2} = M.$$

Then

$$(\Delta\omega - w_g\ \Delta k)^2 - u_g^2\ \Delta k^2 = -\Lambda^2 M u_g\ \Delta k\omega_p. \tag{28}$$

Completing the square gives

$$(\Delta\omega - w_g\ \Delta k)^2 - \left(u_g\Delta k\ - \tfrac{1}{2}\Lambda^2 M\omega_p\right)^2 = -\tfrac{1}{4}\ \Lambda^4 M^2\omega_p^2. \tag{29}$$

For real Δk, from (29), the maximum growth rate is

$$\gamma = \frac{\Lambda^2}{2}\ M\omega_p,$$

which occurs at $u_g\Delta k = \frac{1}{2}\ \Lambda^2 M\omega_p$. From (28), for fixed $\Delta k = -\delta/u_g$, where δ is the frequency mismatch for each half of the plasma dispersion curve,

$$\frac{1}{M}\ \frac{\gamma^2 + \delta^2}{-\delta\omega_p} = \Lambda^2.$$

This is Nishikawa's result[2] generalized to the case when the pump wave vector is

nonzero. Although the growth rate is the same (up to a factor of order unity) as for $k_o = 0$, the low-frequency growing mode can now feed energy into the ion distribution function. It would seem that the previously labeled "nonoscillatory" instability is just a special case of nonlinear Landau damping by coherent waves.

d. Modified Nonoscillatory Instability

Examine the form taken by the nonoscillatory instability for growth rates large compared with the ion-acoustic frequency $k_{(o)}c_S$ but still small compared with the plasma frequency. That is, assume

$$|k_{(o)}c_S| \ll |\omega_{(o)}| \ll \omega_p.$$

Assume also that the LF self-correction is negligible.

$$|\chi\Lambda^2| \ll |1 - K_{(o)}k_{(o)}^2\lambda_{De}^2|.$$

Then (16) reduces to

$$\frac{K_{(1)}}{|\mu_S|^2}\,\frac{K_{(-1)}}{|\mu_A|^2} = -\Lambda^2\left(\frac{K_{(1)}}{|\mu_S|^2} + \frac{K_{(-1)}}{|\mu_A|^2}\right)\left(\frac{K_{(o)}k_{(o)}^2\lambda_{De}^2 - 1}{K_{(o)}k_{(o)}^2\lambda_{De}^2}\right), \tag{30}$$

as for the unmodified nonoscillatory instability. For the growth rates considered here, however, the exact form for $K_{(o)}k_{(o)}^2\lambda_{De}^2$ must be inserted in (30), although the Taylor's series expansions for $K_{(1)}, K_{(-1)}$ are still valid. We now have an equation corresponding to (29):

$$(\Delta\omega - w_g\Delta k)^2 - \left(u_g\Delta k - \tfrac{1}{2}|\mu_S|^2\Lambda^2\omega_p\left(\frac{k_{(o)}^2c_S^2}{k_{(o)}^2c_S^2 - \omega_{(o)}^2}\right)\right)^2 = -\tfrac{1}{4}|\mu_S|^2\Lambda^4\omega_p^2\left(\frac{k_{(o)}^2c_S^2}{k_{(o)}^2c_S^2 - \omega_{(o)}^2}\right)^2. \tag{31}$$

By approximating $|k_{(o)}c_S| \ll |\omega_{(o)}|$ and taking

$$u_g\Delta k = -\tfrac{1}{2}|\mu_S|^2\Lambda^2\omega_p\,\frac{k_{(o)}^2c_S^2}{\omega_{(o)}^2},$$

since $|\Delta\omega| \cong |\omega_{(o)}| \gg |w_g\Delta k|$, (31) becomes

$$\omega_{(o)}^2 \cong \frac{1}{4} |\mu_S|^2 \Lambda^4 \omega_p^2 \frac{k_{(o)}^4 c_S^4}{\omega_{(o)}^4} \tag{32}$$

which has a root

$$\text{Im}\{\omega_{(o)}\} \equiv \gamma = \frac{3^{1/2}}{2^{4/3}} (|\mu_S|\Lambda)^{2/3} \left(\omega_p \omega_{IA}^2\right)^{1/3}, \tag{33}$$

where $\omega_{IA} = k_{(o)} c_S$. This is the modified nonoscillatory instability growth rate. Now, from (32), $|u_g \Delta k| = |\omega_{(o)}|$ so that the assumption $|\Delta\omega| \gg w_g \Delta k$ is justified only if $u_g \gg w_g$; that is, if $|\underline{k}_o| \ll |\underline{k}_B|$. Furthermore

$$\left| \frac{\Delta(\omega_{IA})}{\omega_{IA}(k_B)} \right| \equiv \left| \frac{\Delta k c_S}{k_B c_S} \right| = \left| \frac{\Delta k u_g}{k_B c_S} \right| \left| \frac{c_S}{u_g} \right| = \left| \frac{\omega_{(o)}}{k_{(o)} c_S} \right| \left| \frac{k_{(o)}}{k_B} \right| \left| \frac{c_S}{u_g} \right|$$

which may be large, so that the value of ω_{IA} in (33) may be very different from the unmodified value $k_B c_S$.

References

1. V. P. Silin, Sov. Phys. – JETP 21, 1127 (1965).
2. K. Nishikawa, Phys. Soc. Japan 24, 916 (1968).
3. S. Jorna, Private communication, KMS Fusion, Inc., Ann Arbor, Michigan, August 1973.

VI. APPLIED PLASMA RESEARCH

D. Laser-Plasma Interactions

Academic and Research Staff

Prof. E. V. George
Prof. A. Bers
Prof. H. A. Haus
Dr. A. H. M. Ross
J. J. McCarthy
W. J. Mulligan

Graduate Students

Y. Manichaikul
J. L. Miller
D. Prosnitz
C. W. Werner
D. Wildman

1. CO_2 SHORT-PULSE AMPLIFICATION STUDIES

National Science Foundation (Grant GK-37979X)

A. H. M. Ross

Recent advances in high-pressure gas discharge technology have made possible the deposition of as much as 300 joules/liter in carbon dioxide laser media. Because of the several vibration-rotation degrees of freedom of the CO_2 molecule, this energy is stored in a great many molecular states, and therefore efficient extraction of it requires optical pulse lengths that are large compared with the kinetic collision times governing the energy-exchange processes in the medium. Operation of high-pressure devices as oscillators yields as much as 50 joules/liter from the afterglow of a pulsed discharge, and quasi cw operation has given hundreds of joules/liter in 10-100 μs pulses. Extraction in ns pulses is far less efficient. In this report we summarize theoretical results from a multitemperature kinetic model formulated to describe ns pulse amplification by devices operating at pressures above 1 atm. Numerical results for 1-atm and 5-atm pulse amplifiers are presented.

Amplification of pulses comparable to, or faster than, kinetic collision times requires consideration of the polarization of the molecules, and of inertial effects in the molecular dipoles (for example, see Hopf and Rhodes[1]). Theoretical models incorporating only two vibration states and the full rotation spectrum will be adequate descriptions. If energy is to be extracted efficiently, the pulse length must be several collision times, in which case the coherence effects can be neglected, and the medium can be described by a rate-equation model.

In the rate-equation limit the growth of a plane wave in a transversely uniform medium with nonresonant loss α can be described by a first-order differential equation in distance

$$\left(\frac{\partial I}{\partial z}\right)_{t'} = -\alpha I + \sigma(\omega)\, N_c \left\{ \left[00^\circ 1, J'\right] - \frac{g_{J'}}{g_J} \left[10^\circ 0, J\right] \right\} I, \tag{1}$$

where the stimulated emission cross section is

$$\sigma(\omega) = \frac{\lambda^2}{4\pi t_{sp}} \frac{\Upsilon_{JJ'}^2}{g_{J'}} \frac{\gamma_o}{(\omega-\omega_o)^2 + \gamma_o^2}, \tag{2}$$

with N_c the CO_2 density, g_J the degeneracy of the J^{th} rotational state

$$g_J = 2J + 1, \tag{3}$$

and $[n_1 n_2 n_3, J]$ is the fractional CO_2 population in the state of these quantum numbers (that is, the diagonal element of the density matrix for a single molecule). The spontaneous emission time written here is that for the entire band; an individual line has a matrix element proportional to the rotational matrix element

$$\Upsilon_{JJ'}^2 = \begin{cases} J & \text{for a P(J) line } (J' = J - 1) \\ J + 1 & \text{for an R(J) line } (J' = J + 1) \end{cases} \tag{4}$$

We shall neglect frequency pulling effects, although in high-gain systems they will be important if the input pulse is detuned appreciably.

We assume that the molecular kinetics can be described adequately by rate equations in which only binary collisions are important. Even with the rate-equation model, the six degrees of freedom of the CO_2 molecule in its electronic ground state give rise to so many important vibration-rotation states that the problem would be intractable without further simplifying assumptions. The fact that the molecule is reasonably harmonic in its low vibrational states, and that the interaction of vibration and rotation is weak allows us to treat the relaxation of the various degrees of freedom substantially independently. We also make use of the observation of Osipov and Stupochenko[2] that relaxation of molecular vibrations from a nonequilibrium distribution takes place in two phases: first, a rapid relaxation to quasi equilibrium in which the various normal modes of the molecule acquire a Boltzmann distribution of excitation, which can correspond to a temperature far different from the kinetic temperature of the gas and second, a slow relaxation of these quasi-equilibrium distributions to the kinetic temperature.

Since we are concerned with amplifiers in which the pumping takes place over a time scale that is large compared with the kinetic collision times, it is reasonable to assume that prior to the arrival of the electromagnetic pulse the vibrational states are distributed according to the partial equilibrium distribution

$$[n_1 n_2 n_3] = (1-s)(1-b)^2 (1-a)\, s^{n_1} (n_2+1)\, b^{n_2} a^{n_3}, \tag{5}$$

where s, b, and a are Boltzmann factors for the symmetric stretch, bending, and asymmetric stretch modes (ν_1, ν_2, ν_3) of the CO_2 molecule. We have taken the state $[n_1 n_2 n_3]$ to include all of the states $[n_1 n_2^{\ell} n_3]$, of which there are $n_2 + 1$ (ℓ represents an angular momentum around the symmetry axis of the molecule, and hence can take on the values $-n_2$, $-n_2+2$, $-n_2+4$, ..., n_2-2, n_2).

$$s = \exp\left[-\frac{\epsilon_s}{k_B T_s}\right] \tag{6}$$

$$b = \exp\left[-\frac{\epsilon_b}{k_B T_b}\right] \tag{7}$$

$$a = \exp\left[-\frac{\epsilon_a}{k_B T_a}\right]. \tag{8}$$

The rotation states also reflect a Boltzmann distribution

$$\left[n_1 n_2^{\ell} n_3, J\right] = \left[n_1 n_2^{\ell} n_3\right] 2 g_J \left(\frac{hcB}{k_B T_r}\right) \exp\left[-\frac{hcB}{k_B T_r} J(J+1)\right], \tag{9}$$

where we assume that the rotational constant B is independent of the vibrational state (CO_2 has cB = 11606 MHz and 11698 MHz in the upper and lower laser levels, respectively). Doppler broadening of the laser lines is less than 1% of the homogeneous linewidth at 1 atm, so the velocity distribution of the molecules will be neglected.

Passage of an optical pulse will introduce deviations from these distributions. In particular, a fast pulse will create a "hole" in the state $[00^\circ 1, J']$ (that is, it will depress the population below that given by (5)), and a "peak" in $[10^\circ 0, J]$ because of the stimulated emission process. Judicious approximations allow a description of the kinetics in terms of variables giving the average occupations of the three vibrational modes and the depths of the "holes" in both vibration and rotation. In particular, we assume that the two laser states have the forms

$$[00^\circ 1] = z_v^{-1} a + \alpha \tag{10}$$

$$[10^\circ 0] = Z_v^{-1} s + \beta \tag{11}$$

and that the other states retain their previous occupation probability exclusive of normalization

$$[n_1 n_2 n_3] = Z_v^{-1} s^{n_1} (n_2+1)\, b^{n_2} a^{n_3}, \qquad (n_1 n_2 n_3) \neq \text{laser state}. \tag{12}$$

The normalization condition requires

$$Z_v^{-1} = (1-\alpha-\beta)(1-s)(1-b)^2\,(1-a). \tag{13}$$

Defining the occupation fractions for the individual modes

$$x_q = \sum_{mn} [mnq] \tag{14}$$

$$y_n = \sum_{mq} [mnq] \tag{15}$$

$$z_m = \sum_{nq} [mnq], \tag{16}$$

and with the assumptions (10), (11), and (12), we find the following expressions.

$$\left.\begin{aligned} x_q &= (1-\alpha-\beta)(1-a)a^q, \qquad q \neq 0 \quad \text{or } 1 \\ x_o &= 1 - a - \alpha + (\alpha+\beta)a = (1-\alpha-\beta)(1-a) + \beta \\ x_1 &= (1-\alpha-\beta)(1-a)a + \alpha \end{aligned}\right\} \tag{17}$$

$$y_n = (1-\alpha-\beta)(n+1)b^n \tag{18}$$

$$\left.\begin{aligned} z_m &= (1-\alpha-\beta)(1-s)s^m, \qquad m \neq 0 \quad \text{or } 1 \\ z_o &= 1 - s - \beta + (\alpha+\beta)s = (1-\alpha-\beta)(1-s) + \alpha \\ z_1 &= (1-\alpha-\beta)(1-s)s + \beta. \end{aligned}\right\} \tag{19}$$

These distributions are illustrated in Fig. VI-8.

While this assumption of "holes" in single vibrational states is a convenient approximation, the corresponding ansatz for the rotational distribution is supported experimentally by the work of Cheo and Abrams.[3] They have found that the rotational relaxation may be J-independent and all rotational levels are thermalized in one collision time, so that the expression

$$[00^\circ 1, J'] = [00^\circ 1]\left\{Z_r^{-1}\; 2\; g_{J'} \exp\left[-\left(\frac{hcB}{k_B T_r}\right) J'(J'+1)\right] + \xi\right\} \tag{20}$$

with

$$Z_r^{-1} = (1-\xi)\left(\frac{hcB}{k_B T_r}\right) \tag{21}$$

correctly parametrizes solutions of the model. ξ measures the depth of the "hole" in the rotational sublevel depleted by the radiation; the other levels are populated

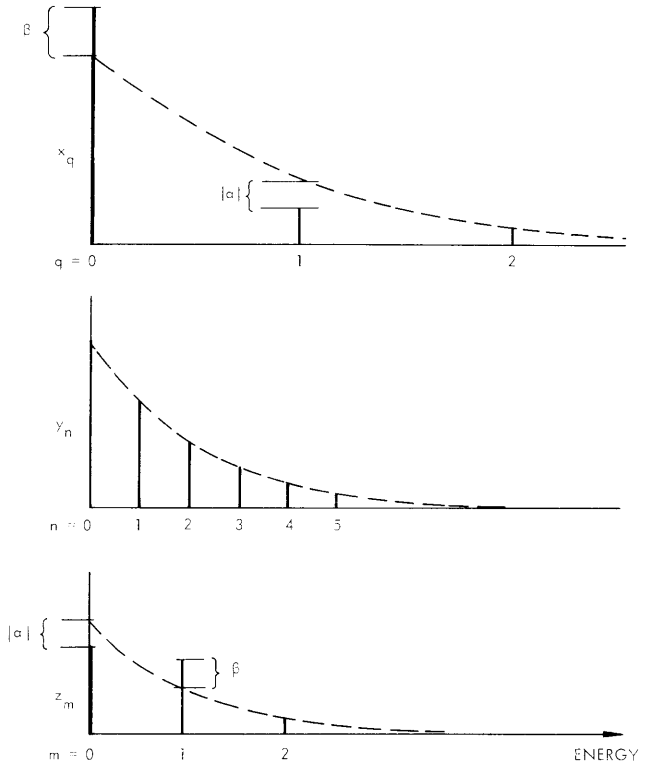

Fig. VI-8. Assumed distributions of CO_2 normal vibrational mode excitations.

in proportion to a Boltzmann distribution scaled in amplitude by $1-\xi$ so that the net vibrational-state population is held constant as ξ varies. A similar expression is assumed for the lower level:

$$[10^\circ 0, J] = [10^\circ 0]\left\{Z_r^{-1}\ 2\ g_J \exp\left[-\left(\frac{hcB}{k_B T_r}\right) J(J+1)\right] + \eta\right\} \tag{22}$$

with

$$Z_r^{-1} = (1-\eta)\left(\frac{hcB}{k_B T_r}\right). \tag{23}$$

This rotational distribution is illustrated in Fig. VI-9.

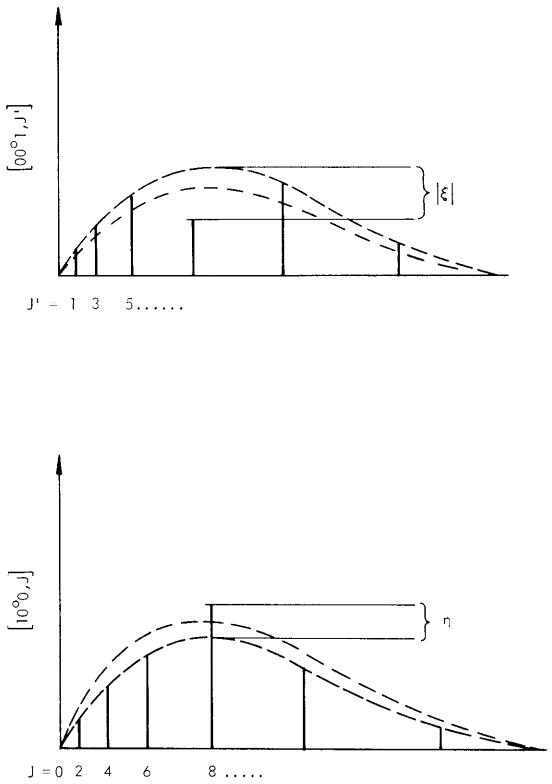

Fig. VI-9. Assumed distributions of CO_2 rotational-state excitations.

The Landau-Teller assumption[4] that the dependence of energy exchange cross sections is that of harmonic oscillator matrix elements can be used to determine the cross sections for the processes to all orders from the measured rates. We have taken into account the following processes.

V-T in the ν_2 mode:

$$(n_1 n_2 n_3) + M \underset{}{\overset{k_b}{\rightleftharpoons}} (n_1, n_2-1, n_3) + M + \epsilon_b$$

Intermode V-V between ν_3 and ν_N:

$$(n_1, n_2+1, n_3) + N_2(v) \overset{k_{an}}{\rightleftharpoons} (n_1 n_2 n_3) + N_2(v+1) + 18\ \text{cm}^{-1}$$

Intermode V-V between ν_3 and $3\nu_2$:

$$(n_1 n_2, n_3+1) + M \overset{k_{ab}}{\rightleftharpoons} (n_1, n_2+3, n_3) + M + .346\ \text{cm}^{-1}$$

Intramode V-V in ν_3:

$$(n_1 n_2, n_3+1) + (n_1' n_2', n_3') \overset{k_{aa}}{\rightleftharpoons} (n_1 n_2 n_3) + (n_1' n_2', n_3'+1)$$

R-T:

$$(j) + M \overset{k_r}{\rightleftharpoons} (j') + M.$$

In addition, the lower laser state has been assumed to have a V-V relaxation of indeterminate nature which has been modeled by a simple exponential decay. Other V-T processes could be included, but the principal loss rate from both ν_3 and ν_N is by the ν_2 mode. Also, because of the close coupling of the ν_1 and ν_2 modes by the Fermi resonance (that is, large cross sections for the conversion of one member of a Fermi resonant pair into the other), we have assumed that the ν_1 and ν_2 vibrational temperatures are equal. The proper variable for the description of the combined bath of states is

$$Q = 2S + B, \tag{24}$$

where S and B are the average occupancies of ν_1 and ν_2:

$$S = \sum_m m z_m = Z_v^{-1} \frac{s}{1-s} + \beta, \tag{25}$$

$$B = \sum_n n y_n = Z_v^{-1} \frac{2b}{1-b}, \tag{26}$$

$$A = \sum_q q x_q = Z_v^{-1} \frac{a}{1-a} + \alpha. \tag{27}$$

For simplicity, we have also assumed $\epsilon_s = 2\epsilon_b$ so that

$$s = b^2. \tag{28}$$

The derivation of the equations for A, N, Q, α, β, ξ, η and the kinetic-rotational energy per particle is straightforward but tedious. Neglecting the $\alpha + \beta$ terms in (17)-(19) compared to 1, we find ($\omega = \omega_o$):

$$\frac{\partial A}{\partial t'} = -R_{an}\left[A(N+1) - (A+1)N\, e^{-\epsilon_{an}/k_B T}\right]$$
$$-R_{ab}\left[1 + \frac{3B}{B+2}\right]\left[A\left(\frac{B}{2}+1\right)^3 - (A+1)\left(\frac{B}{2}\right)^3 e^{-\epsilon_{ab}/k_B T}\right]$$
$$-R_i \tag{29}$$

$$\frac{\partial Q}{\partial t'} = +3R_{ab}\left[1 + \frac{3B}{B+2}\right]\left[A\left(\frac{B}{2}+1\right)^3 - (A+1)\left(\frac{B}{2}\right)^3 e^{-\epsilon_{ab}/k_B T}\right]$$

$$-R_b\left(\frac{B-\bar{B}}{\frac{\bar{B}}{2}+1}\right) + 2R_i \tag{30}$$

$$\frac{\partial N}{\partial t'} = R_{na}\left[A(N+1) - (A+1)N\, e^{-\epsilon_{an}/k_B T}\right] \tag{31}$$

$$\frac{\partial \alpha}{\partial t'} \approx -2R_{aa}\alpha - R_i \tag{32}$$

$$\frac{\partial \beta}{\partial t'} \approx -2R_{bb}\beta + R_i \tag{33}$$

$$\frac{\partial \xi}{\partial t'} = -\gamma_r \xi - (1-\xi)\, R_i/[00^\circ 1] \tag{34}$$

$$\frac{\partial \eta}{\partial t'} = -\gamma_r \eta + (1-\eta)\, R_i/[10^\circ 0] \tag{35}$$

$$\left(\frac{3}{2} + \psi_c + \psi_n\right)\frac{\partial}{\partial t'}(k_B T) = \psi_c \epsilon_b R_b\left(\frac{B-\bar{B}}{\frac{\bar{B}}{2}+1}\right)$$

$$+ \psi_c \epsilon_{an} R_{an}\left[A(N+1) - (A+1)N\, e^{-\epsilon_{an}/n_B T}\right]$$

$$+ \psi_c \epsilon_{ab} R_{ab}\left(1 + \frac{3B}{B+2}\right)\left[A\left(\frac{B}{2}+1\right)^3 - (A+1)\left(\frac{B}{2}\right)^3 e^{-\epsilon_{ab}/k_B T}\right], \tag{36}$$

where

$$\psi_c R_{an} = \psi_n R_{na} = \psi_c \psi_n k_{an} P \tag{37}$$

$$R_{ab} = \sum_M \psi_M k_{ab}^{(M)} P \tag{38}$$

$$R_b = \sum_M \psi_M k_b^{(M)} P \tag{39}$$

$$R_{aa} = \psi_c k_{aa} P \tag{40}$$

$$\bar{B} = B(T_b = T) \tag{41}$$

$$R_i = \sigma(\omega_o)\left\{[00°1, J'] - \frac{g_{J'}}{g_J}\,[10°0, J]\right\}\frac{I}{h\nu}. \tag{42}$$

Equations 1 and 29-36 (which are in the canonical form of a set of hyperbolic equations if t' is the retarded time t - z/c) have been solved numerically for a 30% CO_2 gas mixture at 1 atm and 5 atm total pressure. The input pulse was a 1 ns (FWHM), 1 MW/cm^2 Gaussian shape. Initial conditions were calculated under the assumption of equilibration of Q at T_o, and of $T_a = T_n$ sufficient to give the small-signal gains

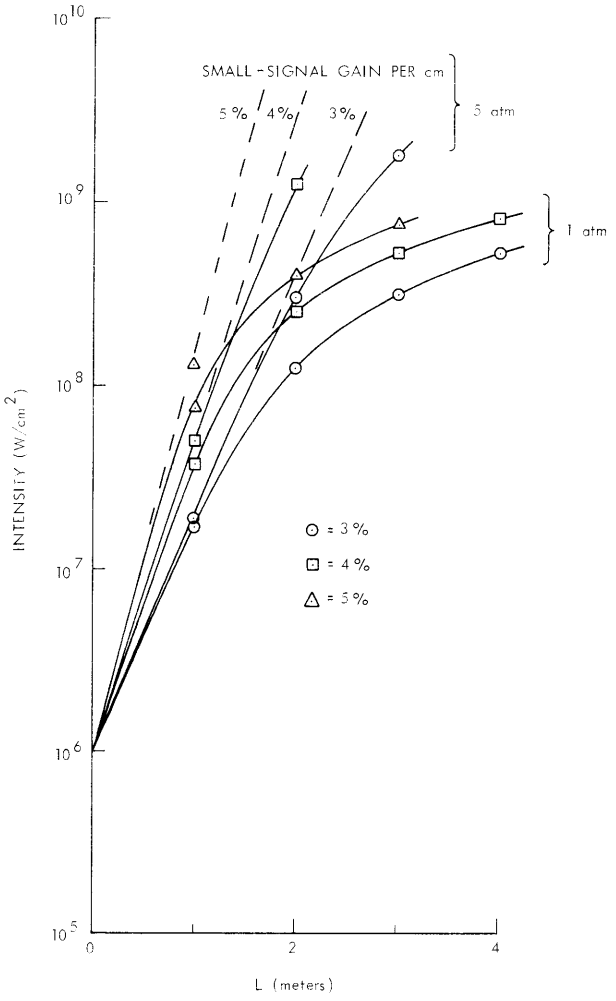

Fig. VI-10. Peak intensity of amplified short pulse in CO_2 media of known small-signal gain at 1 and 5 atm total pressure. Gas mixture: 0.30:0.05:0.65 (CO_2:N_2:He). Input pulse: Gaussian shape, 1 ns FWHM, peak intensity 10^6 W/cm^2.

illustrated; these are typical of those to be expected in various high-pressure discharges. Peak pulse intensity as a function of depth in the amplifier is shown in Fig. VI-10, and the output pulse shapes are shown in Fig. VI-11.

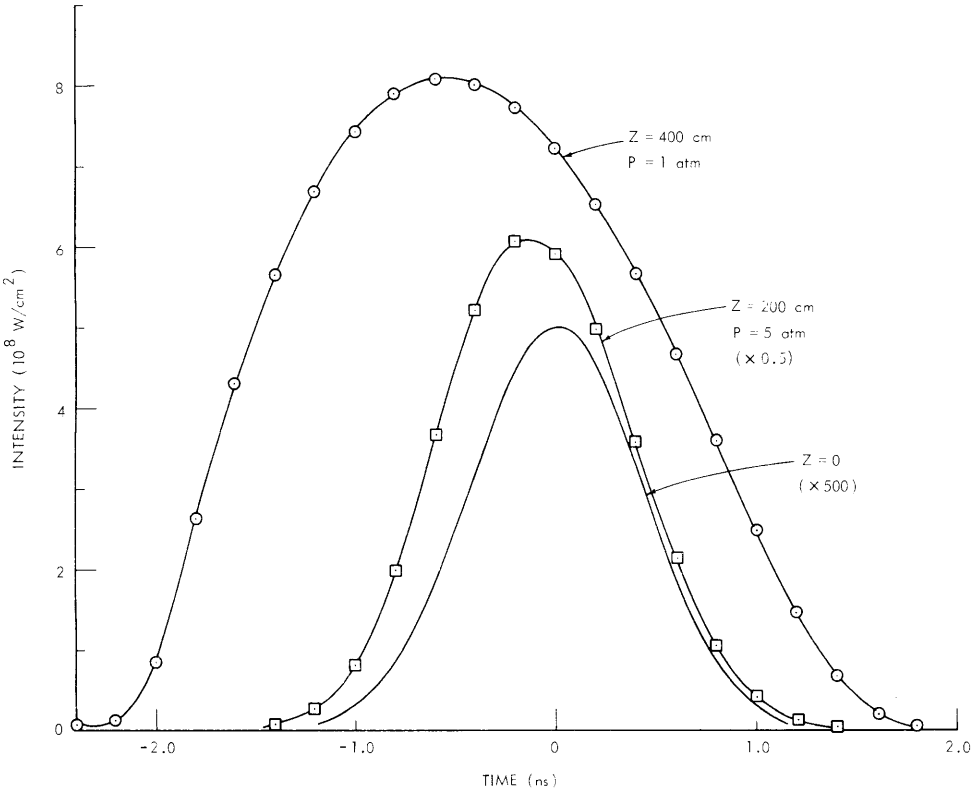

Fig. VI-11. Temporal pulse profiles for amplifiers of Fig. VI-10, 4%/cm small-signal gain at 1 atm, 3%/cm at 5 atm.

Note that there is substantial broadening of the pulse at 1 atm, while at 5 atm the output is a reasonably faithful diplicate of the input, even after amplification by more than 1000 in intensity. Note also the extremely large saturation intensity at 5 atm; elementary considerations of the saturation process show that it should scale approximately as the square of the total pressure.

References

1. F. A. Hopf and C. K. Rhodes, "Influence of Vibrational, Rotational, and Reorientational Relaxation on Pulse Amplification in Molecular Amplifiers," Phys. Rev. A 8, 912-929 (1973).

2. A. I. Osipov and E. V. Stupochenko, "Non-equilibrium Energy Distributions over the Vibrational Degrees of Freedom in Gases," Sov. Phys. —Usp. 6, 47-66 (1962).

3. P. K. Cheo and R. L. Abrams, "Rotational Relaxation Rate of CO_2 Laser Levels," Appl. Phys. Letters 14, 47-49 (1969).
4. K. F. Herzfeld and T. A. Litovitz, Absorption and Dispersion of Ultrasonic Waves (Academic Press, Inc., New York, 1959).

2. AMPLIFICATION OF TWO HIGH-INTENSITY NANOSECOND TEA CO_2 LASER PULSES (AHN)

National Science Foundation (Grant GK-37979X)
U. S. Army – Research Office – Durham (Contract DAHC04-72-C-0044)

Y. Manichaikul

Experiment

We have previously reported on the generation and amplification of high-intensity nanosecond pulses.[1] Two or three of these pulses were produced. They were from the P(16) transition, 2 ns wide (FWHM), separated by 12 ns. When these pulses were focused into a three-electrode laser amplifier as shown in Fig. VI-12, a peak intensity of 2-3 MW/cm^2 was obtained. A beam splitter was used so that the intensity of the pulses could be monitored. The input and output detectors were as shown in Fig. VI-12. In this experiment the detected input signals were delayed 100 ns by using 60 ft of

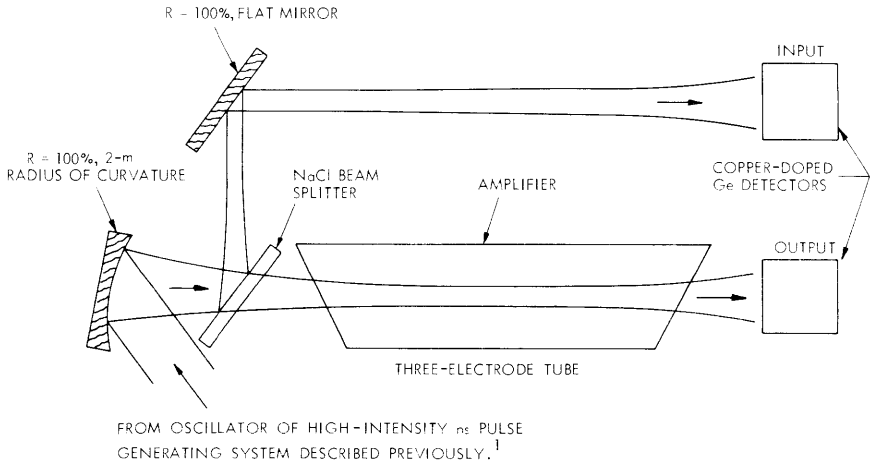

Fig. VI-12. Experimental arrangement for amplification of high-intensity ns pulses. (See Y. Manichaikul.[1])

RG-8 cable. The add mode of a Tektronix oscilloscope was used to display the signals for both input and output pulses on the same screen. The two detectors were calibrated against each other by comparing the oscilloscope picture of the input and output pulses without discharge exciting the three-electrode laser amplifier. Figure VI-13a shows

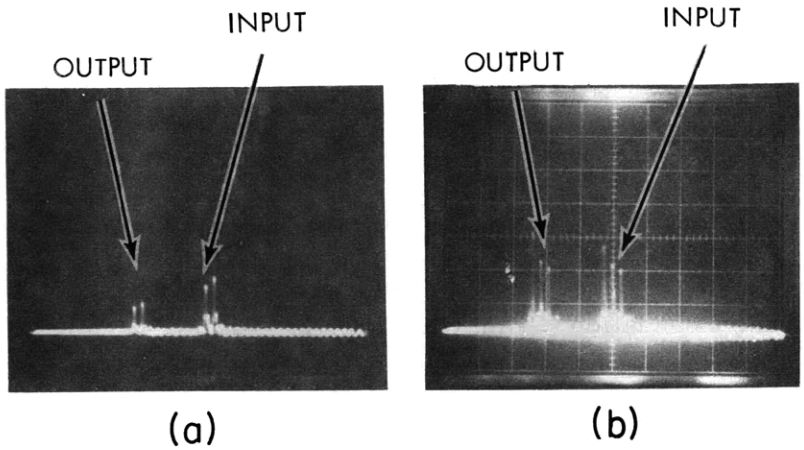

Fig. VI-13. Output and input of AHN experiment. Total pressure: 200 Torr. Gas mixture: CO_2:N_2:He = X:4:100. Intensity of input pulse: 0.75 (MW/cm^2)/div. Intensity of output pulse: 1.12 (MW/cm^2)/div. Time: 50 ns/div. (a) Amplifier off. (b) Amplifier on.

the oscilloscope display for this case.

In order to probe the temporal evolution of the three-electrode laser amplifier, we first fired the amplifier and, after a chosen delay time, the oscillator. In general, the oscillator was fired ~30 μs after the onset of the discharge in the amplifier for two reasons: first, we wished to avoid the effects on our measurements of the shock waves generated by the discharge. Second, we wished to be certain that the symmetric stretching (SS) and bending (B) modes of CO_2 had equilibrated with each other at slightly above the kinetic temperature of the gas.[2]

Measurements on the amplification of high-intensity ns pulses were made at 200 Torr of CO_2:N_2:He mixtures. The ratio of these mixtures was CO_2:N_2:He = X:4:100, where CO_2 partial pressure was varied from 3.5 to 35 Torr partial pressure. Small-signal gain of this three-electrode laser amplifier in each case was measured by a cw CO_2 laser.

Results

Figure VI-13b illustrates the input and output pulses when the amplifier is turned on. Four such measurements were made and their average was taken at each CO_2 partial pressure studied. We have found that the RG-8 cable used for the time delay introduces some distortion in the input signals. This distortion can be accounted for if the first (second) pulses of the input and output pulses from the amplification measurements are compared with the first (second) pulses of the input and output pulses when the amplifier was evacuated.

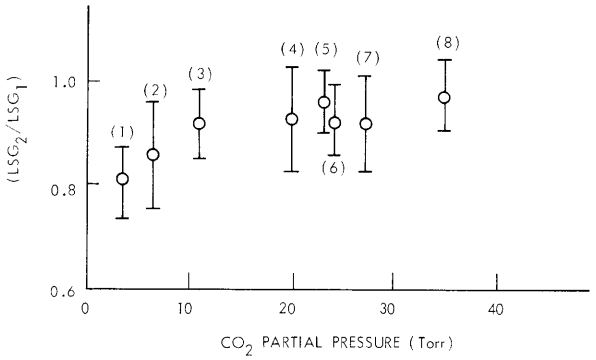

Fig. VI-14. LSG_2/LSG_1 vs partial CO_2 pressure.

Table VI-1. Experimental results.

No.	P_{CO_2} (Torr)	SSG ±10%	LSG_1 ±10%	T_{vv}^a (°K)	$\frac{\Delta N_u}{N_u(0)}$
1	3.5	0.50	0.30	1180	0.12
2	6.5	0.70	0.36	1150	0.11
3	11.0	1.50	0.76	1155	0.14
4	20.0	1.00*	0.52	845	0.11
5	23.0	1.50*	0.75	860	0.13
6	24.0	2.00*	0.96	890	0.14
7	27.0	2.50*	1.15	935	0.15
8	35.0	2.00	0.81	830	0.10

Notes: *Not measured directly; calculated from LSG_1 and the peak intensity of the pulse.

SSG = $\frac{I_{in} - I_{out}}{I_{in}}$ is the small-signal gain across the tube. Here the intensity is less than 1 W/cm^2.

LSG_1, large-signal gain of the first pulse.

T_{vv}^a, temperature of the asymmetric stretching mode calculated from SSG.

$\frac{\Delta N_u}{N_u(0)}$, fractional depletion of the 00°1 population by an ns pulse.

ΔN_u, calculated from the large-signal gain and the intensity of the pulse.

$N_u(0)$, obtained from SSG.

Figure VI-14 shows LSG_2/LSG_1 vs the partial pressure of CO_2 studied. We have

$$LSG_i \triangleq \frac{I_{out\,i} - I_{in\,i}}{I_{in\,i}},$$

where i = 1, 2, with 1 and 2 representing first and second pulses. LSG_1 (LSG_2) is the large-signal gain of the first (second) pulses. The following observations can be made from these measurements. (i) LSG_2/LSG_1 is less than unity. This is to be expected, since the first pulse had depleted a fraction of the population from the 00°1 level of CO_2. (ii) The ratio LSG_2/LSG_1 is approximately 0.8 at CO_2 partial pressure of 3.5 Torr and the ratio increases slowly to 0.9 as CO_2 partial pressure increases to 20 Torr or higher, which is as expected, since the 00°1 level of CO_2 was being repopulated by the higher $O\,n^{\ell}m$ levels at a rate[3] that is directly proportional to the CO_2 partial pressure.

Table VI-1 gives other experimental results of interest. We found that the large-signal gain of our pulses is approximately one-half the small-signal gain, and the fractional depletion of the 00°1 level, $\frac{\Delta N_u}{N_u(0)}$, is between 0.10 and 0.15.

A theoretical model for the amplification of high-intensity nanosecond pulses is being developed. We shall present the theory, and make a comparison of theory and experiment in a future report.

References

1. Y. Manichaikul, "Generation and Amplification of High-Intensity, Nanosecond TEA CO_2 Laser Pulses," Quarterly Progress Report No. 110, Research Laboratory of Electronics, M.I.T., July 15, 1973, pp. 118-121.
2. D. L. Lyon, IEEE J. Quant. Electronics, Vol. QE-9, No. 1, pp. 139-153, January 1973.
3. I. Burak, Y. Noter, and A. Szöke, IEEE J. Quant. Electronics, Vol. QE-9, No. 5, pp. 541-544, May 1973.